Acta Astronautica 128 (2016) 160–179

Contents lists available at ScienceDirect

Acta Astronautica

journal homepage: www.elsevier.com/locate/aa

Aquarius, a reusable water-based interplanetary human spaceflight transport

Daniel R. Adamo [a,*,1], James S. Logan [b,2]

[a] Independent Astrodynamics Consultant, Salem, OR 97306, USA
[b] Space Enterprise Institute, Austin, TX 78759, USA

ARTICLE INFO

Article history:
Received 27 January 2016
Received in revised form
6 July 2016
Accepted 19 July 2016
Available online 20 July 2016

ABSTRACT

Attributes of a reusable interplanetary human spaceflight transport are proposed and applied to example transits between the Earth/Moon system and Deimos, the outer moon of Mars. Because the transport is 54% water by mass at an interplanetary departure, it is christened *Aquarius*. In addition to supporting crew hydration/hygiene, water aboard *Aquarius* serves as propellant and as enhanced crew habitat radiation shielding during interplanetary transit. Key infrastructure and technology supporting *Aquarius* operations include pre-emplaced consumables and subsurface habitat at Deimos with crew radiation shielding equivalent to sea level on Earth, resupply in a selenocentric distant retrograde orbit, and nuclear thermal propulsion.

1. Introduction

Consider evolution of in-space nuclear thermal propulsion (NTP) technology to the point where fission reactor core temperatures exceeding 3000 °C can be achieved during major translational maneuvers (burns). Under these conditions, water molecules pumped into the core will disassociate into hydrogen and oxygen atoms, and specific impulse I_{SP} near 1000 s could be achieved.[3] This level of efficiency, twice that attainable with chemical propulsion, dramatically reduces total mass for an interplanetary transport of specified payload mass.[4]

When high propulsive efficiency is achieved with water as propellant, the practicality of interplanetary human spaceflight is enhanced in multiple respects. First, liquid water is easily stored for months or years without exotic thermal conditioning burdens imposed by cryogens or toxicity hazards associated with hypergols. Second, liquid water stored about the crew habitat to support arrival propulsion requirements at an interplanetary destination also serves as an effective radiation shield during interplanetary transit. Third, water is arguably the most common volatile to be found on small bodies such as asteroids and minor moons throughout our solar system, leading to the promise of in-situ resource utilization (ISRU). With ISRU producing water for propulsion, radiation shielding, and hydration/hygiene near an interplanetary destination, mass to be transported there from Earth in support of crew return is virtually eliminated.

Significant radiation shielding is essential for routine interplanetary human spaceflight [1]. Direct radiation measurements by multiple investigators over extended time periods on the Space Shuttle [2], inside/outside International Space Station [3] and with multiple sensors embedded in a phantom torso [4], lunar orbit [5], Mars orbit [6], interplanetary transit [7], and on the Martian surface [8] have substantiated consistent, often alarming, exposure scenarios. Space is a seething cauldron of ionizing radiation emanating from all directions simultaneously, modulated only slightly by solar wind and punctuated intermittently by potentially enormous coronal mass ejections [9]. This paper advocates a combination of spacecraft equipment and consumables placement relative to crew, innovative mission architecture elements (habitat location, multi-use propellant), and feasible mass shielding enhancements during transit. These mitigation techniques reduce total mission exposures by more than 67%, from 1.2 Sv to less than 0.4 Sv.

A synergistic consequence of interplanetary arrival propellant doubling as a crew habitat radiation shield is transport reusability. In an Earth return transit from interplanetary space, discarding the transport while its crew undergoes direct atmospheric entry and landing becomes absurd if radiation shielding can instead be

* Corresponding author.
E-mail address: adamod@earthlink.net (D.R. Adamo).
1 Sole proprietor, 8119 Kloshe Ct. S.
2 Co-Founder, 3407 Steck Ave.

3 Personal communication with Dr. James A. Dewar, U.S. Department of Energy, Retired, on 29 September 2010.

4 It is beyond the scope of this paper to document mature technology achieving I_{SP} near 1000 s using water propellant. Rather, the paper aims to encourage development of such technology by illustrating in detail how it enables routine interplanetary human spaceflight. Although NTP appears to be the most direct route to the goal of efficient water-based propulsion, this approach is at best the result of informed speculation.

http://dx.doi.org/10.1016/j.actaastro.2016.07.026
0094-5765/

Nomenclature

c_{DAC}	docking/airlock/centrifuge module mass-to-volume ratio m_{DAC}/V_{DAC}
c_H	crew habitat module mass-to-volume ratio m_H/V_H
c_{RCS}	mass ratio $m_{RCS}/(m_P+m_S)$
c_T	mass ratio $m_T/(m_P+m_S)$
g	Earth surface gravity acceleration$=$0.00980665 km/s^2
m_A	miscellaneous stowage mass in pressurized volumes accessible to the crew, including the crew itself
m_B	budgeted propellant mass
m_C	centrifuge mass
m_{DAC}	docking/airlock/centrifuge module mass, excluding m_A and m_C
m_H	crew habitat module mass, excluding m_A and m_{LS}
m_J	mass of water jacketing the crew habitat module sufficient to provide marginally adequate crew radiation shielding (composed of m_S and typically a portion of m_P)
m_{LS}	mass associated with crew environmental control and life support systems consumables
m_{LS}'	m_{LS} loaded at a transit departure when $T=0$
m_{NTP}	nuclear thermal propulsion system mass, excluding m_P and m_T
m_P	nominally usable water propellant mass
m_{RCS}	attitude control propellant mass
m_S	mass of water dedicated to crew habitat radiation shielding and usable as propellant only to address contingencies
m_T	structural mass of water tank holding m_P and m_S
m_{TOT}	total *Aquarius* mass
m_Z	total of static *Aquarius* mass components for use in the rocket equation
r_0	a stable selenocentric orbit's mean radius over time
v_X	exhaust speed
v_∞	asymptotic speed
A	ratio of fully loaded *Aquarius* mass before to mass after 1.05 $\Delta v'$ is expended by nuclear thermal propulsion
B	ratio of fully loaded *Aquarius* mass before to mass after 1.05 $\Delta v_D'$ is expended by nuclear thermal propulsion
F	propulsive thrust
I_{SP}	specific impulse
T	elapsed time since transit departure
V_{DAC}	total docking/airlock/centrifuge module volume
V_H	total crew habitat module volume
V_{H+}	volume containing crew habitat module and a surrounding jacket of radiation shielding water
ρ_A	area density used to quantify radiation shielding mass about a specified volume's external surface area
Δt	interplanetary transit time from departure to arrival
$\Delta t'$	maximum Δt among interplanetary transits documented in Section 3.
Δv	change-in-velocity magnitude
Δv_C	second interplanetary transit abort Δv achieving capture at the departure planet
Δv_D	tally of Δv values for a transit's departure burns only
$\Delta v_D'$	maximum Δv_D among interplanetary transits documented in Section 3.
Δv_R	first interplanetary transit abort Δv commencing return to the departure planet
$\Delta v'$	maximum total Δv among interplanetary transits documented in Section 3.

expended as propellant to deliver the crew to safe haven at an orbital destination where the transport is resupplied. With reuse, over 100 metric tons (t) of transport structure mass are thereby recycled before the next interplanetary departure. This mass includes costly systems that need not be fabricated, launched, and assembled in space for but a single mission. Specialized crew systems required to withstand Earth atmospheric entry and landing are superfluous in the context of an indirect crew return mission profile. These systems have a mass exceeding 10 t and need not be hauled out to an interplanetary destination before Earth return months or years later when their critical functions are at long last required.

An indirect Earth return from interplanetary space may be the only option for crew survival. Atmospheric accelerations following Earth entry speeds of at least 11 km/s after an interplanetary transit have proved to be survivable for humans only in the context of Apollo Program missions whose crews were de-conditioned by microgravity for at most two weeks beforehand [10]. In a typical Earth return interplanetary transit, the crew is subjected to microgravity for at least several months.[5]

With these primary motivations in mind, a reusable NTP-powered interplanetary transport utilizing water as propellant and as radiation shielding for its crew is proposed and documented. Additional water for open-loop crew hydration and hygiene brings this transport's gross mass to slightly more than half water immediately prior to an interplanetary departure. She is therefore christened *Aquarius* in deference to the Zodiacal Water-Bearer of that name.[6]

To demonstrate *Aquarius* performance and supporting infrastructure functions, her first three interplanetary transits are documented. Transit 1 begins in the elliptical Earth parking orbit (EEPO) where *Aquarius* has undergone assembly and ends at rendezvous with the outer martian moon Deimos, arguably the optimal location for human tele-robotic exploration of Mars [11]. The crew conducts this exploration from a sub-surface Deimos habitat while *Aquarius* is resupplied for Transit 2 using pre-emplaced consumables cached there (via Deimos ISRU or robotically transported cargo) before Transit 1 began. Transit 2 departs Deimos and ends in a stable selenocentric distant retrograde orbit (SDRO) with mean radius $r_0=$12,500 km, as would all future transits from Deimos until *Aquarius* is decommissioned. At this point, *Aquarius* has docked with SDRO-resident infrastructure for Transit 3 resupply while her first crew is replaced. Transit 3 begins in the SDRO and ends at Deimos, as would all future transits to Deimos until *Aquarius* is decommissioned. An SDRO appears to be the closest stable orbit to Earth in which a reusable spacecraft can be serviced between interplanetary transits without expending excessive change-in-velocity Δv [12,13, Section 2.2]. As a further example, *Aquarius* return to Earth abort capability is estimated after Transit 3 enters interplanetary space.

[5] It has been argued that crew survival during direct Earth atmospheric entry following an interplanetary mission months or years in duration can be ensured with the proper entry vehicle design. Until such a design is proven with appropriately de-conditioned crews during a series of progressively more stressful flight tests, a prudent and responsible interplanetary mission profile will avoid crew direct Earth return. Without relevant flight test experience, a *calculated* risk becomes an unacceptable *blind* risk to crew safety.

[6] A male gender is usually associated with The Water-Bearer in mythology and astrology. But precedent refers to transports with feminine pronouns even in gender-neutral cases such as *Enterprise* or *Endeavor*. This feminine attribute will therefore be applied to *Aquarius* as well.

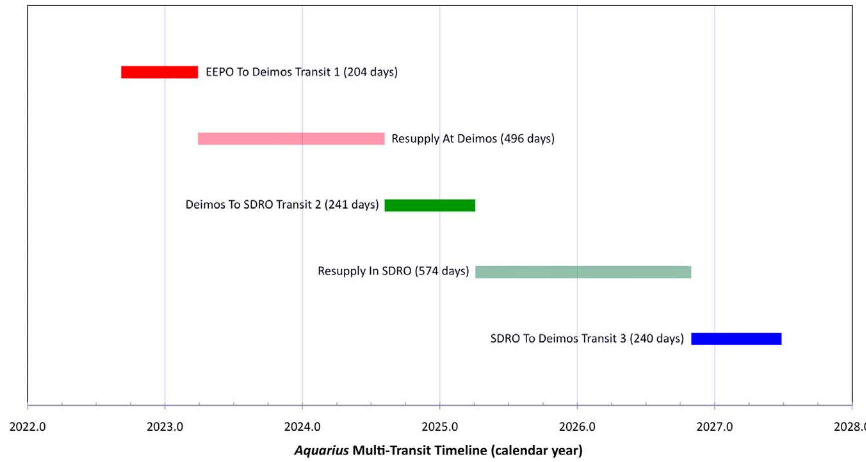

Fig. 1. The first three interplanetary transits to be flown by *Aquarius*, together with intervening loiter periods at Deimos and in SDRO, fall within the 2020s decade. Although this timeline is likely premature with respect to the pace of interplanetary human spaceflight technology development, years spanned by it encompass some of this century's most challenging Earth/Mars transit cases from a performance perspective. Demonstrated viability with respect to these performance-challenged transits therefore tends to render *Aquarius* capable of routinely handling any transit between SDRO and Deimos. Note that an *Aquarius* sister transport could depart Earth's vicinity for Deimos at about the time Transit 2 begins.

By demonstrating practical roundtrips to Deimos, *Aquarius* capability delivering human explorers to more than 1100 near-Earth asteroids (NEAs) is inferred [14]. Although NEA destinations are generally more accessible than Deimos because of reduced total Δv and transit time Δt, practical human spaceflight roundtrip opportunities to a particular NEA are generally less frequent than those to Deimos. Even if *Aquarius* never visits an NEA, supporting ISRU capability is offered by water-rich NEA material (raw or pre-processed in-situ) robotically transported to infrastructure near *Aquarius* transit termini [15].

2. Interplanetary transit assumptions

Each of the following paragraphs documents an assumption and rationale relating to capabilities of *Aquarius* or her supporting infrastructure. Together, these enable interplanetary transits between EEPO/SDRO and Deimos. A unique 3-character code with format **Axx** or **Bxx**, where **xx** is a sequential 2-digit integer, initiates each paragraph to aid concise referencing. An **Axx** code relates primarily to *Aquarius*, and a **Bxx** code relates primarily to supporting infrastructure.

A01: *Aquarius* will fly roundtrips to Deimos in accord with a conjunction mission profile. This entails spending about 500 days at Deimos while Earth phases through a solar superior conjunction observed from Mars before an Earth return transit can begin. With protracted time at Deimos, significant tele-robotic Mars exploration can be conducted by the crew to justify risks in sending them so far from Earth. The Deimos loiter interval is also of sufficient duration to ensure *Aquarius* resupply from pre-emplaced resources, whether they originate on Deimos through ISRU or on Earth through robotic transport.

A02: *Aquarius* will fly short-way (Type 1) transits to reduce time spent in interplanetary space with respect to alternative long-way (Type 2) transits. A short-way transit requires about 200 to 240 days to complete. Reducing transit duration by excluding long-way trajectories also reduces undesirable crew exposure to radiation and micro-gravity.

A03: radiation shielding to an area density $\rho_A > 51.5$ g/cm^2 will be provided throughout the crew habitat module (Hab) aboard *Aquarius* except during intervals less than 100 h required to reach crew safe haven during arrival at an interplanetary destination. At 51.5 g/cm^2, Hab shielding is 5% of the 1030 g/cm^2 provided by Earth's atmosphere at sea level and is called "radiation protection 5" (RP5) shielding. This shielding "jacket" has two components. Hab structure is assumed to provide 14.5 g/cm^2, and water surrounding this structure is assumed to provide the remaining 37.0 g/cm^2. The RP5 specification is assumed sufficient to satisfy radiation exposure standards during short-way transits from Earth to Deimos and back (per A01 and A02) for any adult astronaut [16]. Exposure rates no greater than on Earth's surface (RP100) are further assumed during Deimos loiter between transits (per B01).

A04: to effect safe rendezvous as an interplanetary destination is approached, *Aquarius* must consume water propellant to the point Hab shielding is less than RP5 (per A03). Under these conditions, extra water propellant will be expended in the interest of expediting crew arrival at safe haven from radiation exposure beneath the surface of Deimos (per B01) or at SDRO-resident infrastructure (per B02). Near the end of a transit, this overriding interest will generally result in propellant expenditure that is *not* minimal.

A05: the NTP system aboard Aquarius has $I_{SP}=900$ s, exhaust speed $v_X=g\ I_{SP}=8.826$ km/s, and develops a total thrust $F=333{,}617$ Nt from three engines [17], p. 25. Fission reactors powering these engines are also capable of powering all electrical loads aboard *Aquarius* during cruise periods (called "bi-modal" reactor operation in [13], Section 3.1). During NTP burns, a partial power-down of nonessential electrical loads may be necessary. Mass of NTP systems (excluding usable water propellant mass m_P and water tank structural mass m_T) $m_{NTP}=41{,}700$ kg ([17], Table 4–1, p. 27). On p. 26 of [17], the assumed value of m_{NTP} is associated with fission reactor radiation shielding mass not required on a cargo mission. From Table 4–1, the equivalent cargo mission mass is 8 t less than m_{NTP}, indicating shielding in that amount is provided for *Aquarius*.

A06: the mass ratio of *Aquarius* attitude control propellant to NTP propellant plus dedicated Hab radiation shielding water $c_{RCS}=m_{RCS}/(m_P+m_S)=4.9/59.7=0.0820770$ [17], p. 27. Because an attitude timeline during *Aquarius* transits is beyond the scope of this study, m_{RCS} is not depleted from its initial interplanetary departure value as a conservative assumption when *Aquarius* transits are assessed in Section 6.

A07: the mass ratio of water tank structure to NTP propellant plus dedicated Hab radiation shielding water $c_T=m_T\ /\ (m_P+m_S)=14.0/73.1=0.191518$ [17], p. 27.

A08: the Hab mass-to-volume ratio is that of the ISS *Destiny* lab module $c_H=m_H/V_H=24{,}023/(\pi{*}2.15^2{*}9.2)=179.809$ kg/m^3 [18].

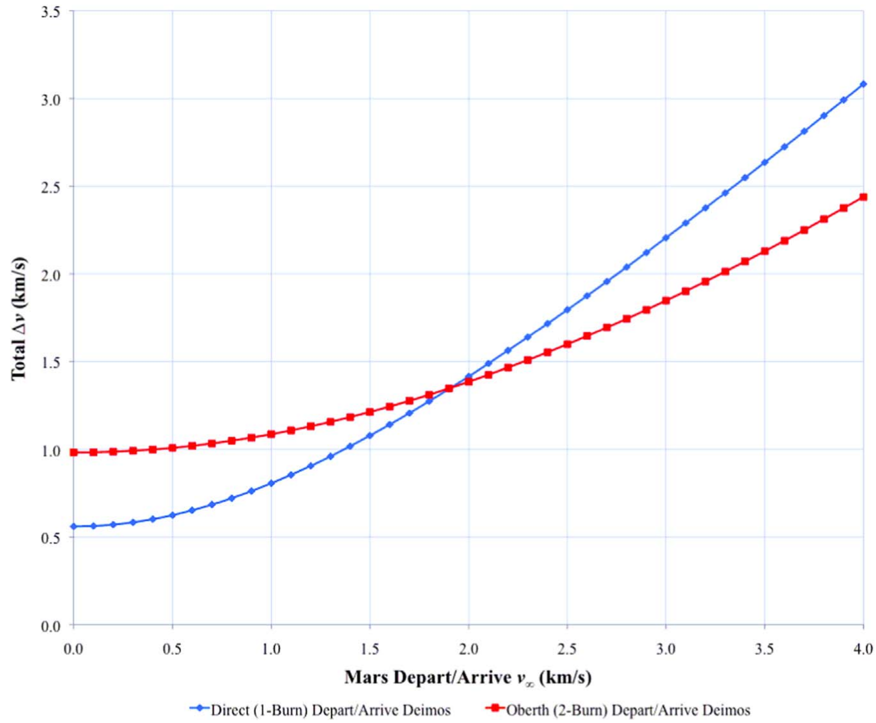

Fig. 2. Total impulsive Δv required to depart from or arrive at the Deimos terminus of an interplanetary transit (assuming a depart/arrive asymptote in the Mars-centered Deimos orbit plane) is plotted as a function of the associated Mars asymptotic speed v_∞ for two trajectory design strategies. When $v_\infty > 2.0$ km/s, the 2-burn Oberth strategy (red squares) requires less total Δv than does the 1-burn Direct strategy (blue diamonds). All three Deimos departures/arrivals documented in this section have $v_\infty > 3$ km/s and therefore utilize the Oberth strategy in their trajectory designs. (For interpretation of the references to color in this figure legend, the reader is referred to the web version of this article.)

Table 1
Transit 1 burns are summarized as *Aquarius* departs EEPO and arrives at Deimos. The leftmost column provides the date and universal time (UT) of each event in the rightmost column. Values in the Δv column are positive for prograde burns and negative for retrograde burns. A total Δv=3.695 km/s is expended over Δt=204 days during Transit 1 with Δv_D=1.358 km/s.

Date @ UT	Δv (km/s)	Event
2022 Sep 08 @ 02:01	−0.242	Lower perigee height from +7725 km to +400 km
2022 Sep 09 @ 00:00	+1.116	Trans-Mars injection (TMI)
2023 Mar 30 @ 20:00	−1.586	Mars orbit insertion (MOI)
2023 Mar 31 @ 02:00	+0.751	Deimos rendezvous

A09: *Aquarius* will transport a crew of 3.

A10: the Hab is a cylinder 2.3 m in radius and 12.2 m in length with a total volume $V_H = \pi * 2.3^2 * 12.2 = 202.752$ m^3. Although pressurized Hab volume will be somewhat less than V_H, the total volume for each crewperson is 202.752/3 = 67.584 m^3 (per A09). This is 3.38 times the 20 m^3 NASA standard for "Optimal" per capita habitable volume at Δt=6 months or more ([19], Fig. 8.6.2.1–1).

A11: the Hab has mass $m_H = 179.809 * 202.752 = 36{,}457$ kg (per A08 and A10). If m_H is distributed uniformly within the Hab, it contributes $\rho_A = 36{,}457 / (2*\pi*2.3^2 + 2*\pi*2.3*12.2) = 173.982$ kg/m^2 = 17.4 g/cm^2 to Hab radiation shielding (per A10), indicating the assumed Hab structure shielding component of 14.5 g/cm^2 is adequate (per A03). Note that a component of m_T also serves to shield crew in the Hab from radiation, but this contribution is ignored as an additional conservative (and simplifying) assumption.

A12: water mass jacketing the Hab exterior must provide an area density of 37 g/cm^2 (per A03). A cylinder exceeding Hab length by 74 cm and Hab radius by 37 cm has a volume $V_{H+} = \pi * 2.67^2 * 12.94 = 289.806$ m^3 (per A10). Thus, the volume $V_{H+} - V_H = 289.806 - 202.752 = 87.053$ m^3 jackets the Hab with liquid water sufficient to shield the crew (per A03). This jacket is maintained in uniform thickness with a pressurized bladder similar to those ensuring forward ullage for in-space propellant tanks. Liquid water has a density of 1000 kg/m^3. Therefore, the Hab's shielding water jacket has mass $m_J = 1000 * 87.053 = 87{,}053$ kg. Until NTP burns commence near an interplanetary transit's destination, $m_S + m_P > m_J$ (per A03).

A13: environmental control and life support systems (ECLSS) consumables are dumped/vented overboard *Aquarius* in open-loop fashion for simplicity and reliability. Crew per capita ECLSS consumables mass depletion rates are 29.26 kg/day of water (stowed in a dedicated reservoir distinct from that holding m_P and m_S), 0.82 kg/day oxygen, 0.72 kg/day dehydrated food, 0.69 kg/day miscellaneous supplies, 0.69 kg/day atmospheric losses, and 0.69 kg/day ECLSS maintenance. These allocations are relatively liberal with respect to others considered state-of-the-art [20].[7] The entire crew therefore consumes a total ECLSS mass of 98.61 kg/day (per A09). Total ECLSS mass to be loaded for a transit has a 5% margin such that $m_{LS}' = 1.05 * \Delta t' * 98.61$ kg initially, where the maximum transit time $\Delta t'$ among transits documented in Section 3 is measured in days. If T is measured in days, ECLSS consumables mass at any time during transit is $m_{LS} = m_{LS}' - T * 98.61$.

A14: miscellaneous mass stowed aboard *Aquarius* in pressurized volumes accessible to the crew includes ([17], p. 34) crew accommodations (4210 kg), extravehicular activity systems

[7] For example, the A13 per capita water allocation is over 8 times that on [20], p. 7 and 4 times the nominal allocation on [20], p. 9. However, ISS per capita water *usage* (the amount *consumed* if ISS had open-loop ECLSS consistent with A13) is 28.63 kg/day ([20], p. 12), 98% of A13's daily per capita water budget. Allocations for A13 are therefore considered plausible in an open-loop ECLSS context.

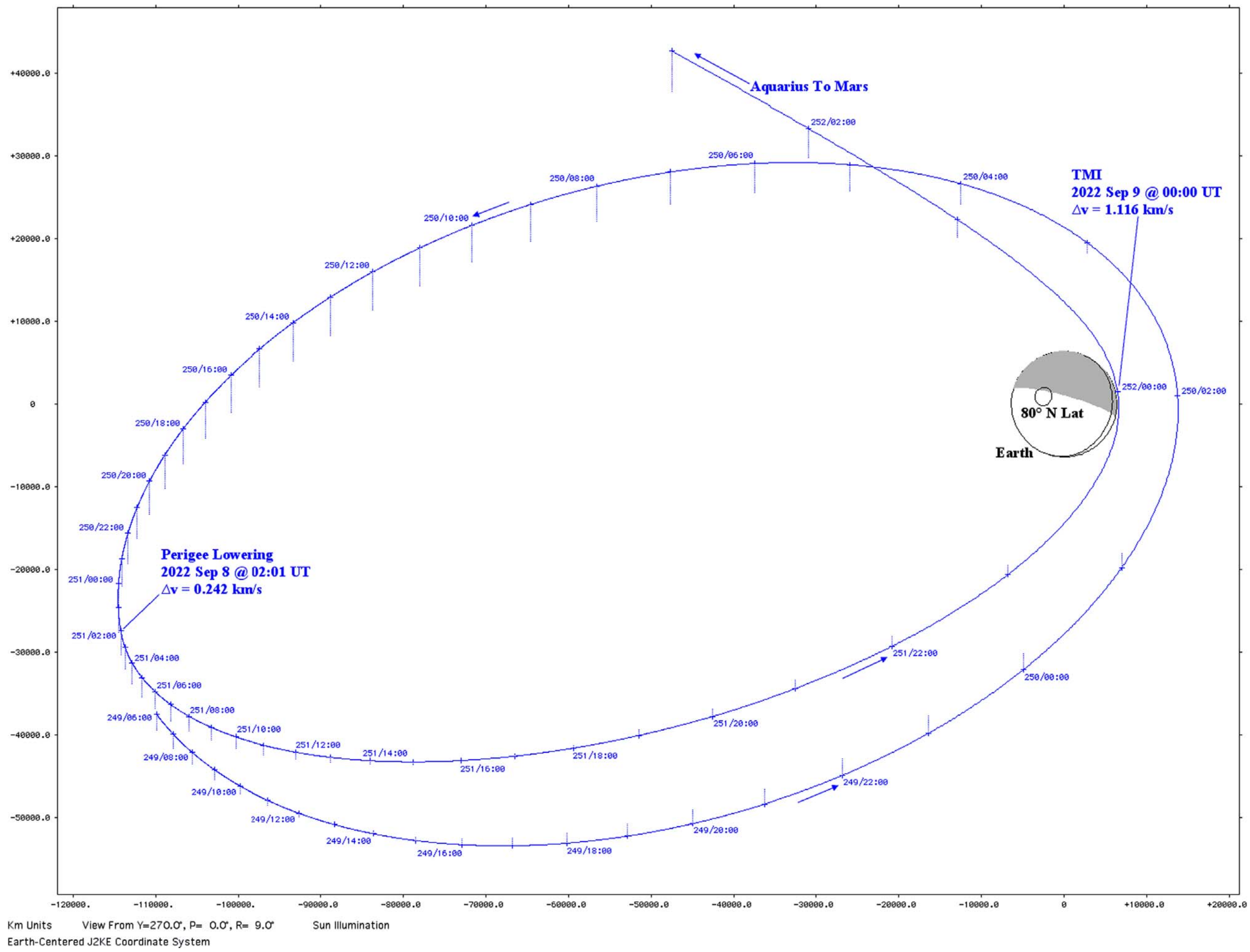

Fig. 3. Geocentric inertial *Aquarius* motion is plotted from her last EEPO through perigee lowering and TMI burns as she departs Earth for Mars and Deimos rendezvous. The plot plane nearly coincides with the plane of *Aquarius* motion. Time tick labels are 2022 September 6–9 UT in day-of-year (DOY)/hh:mm format. Dotted lines are projections onto the ecliptic plane, and the shaded area is Earth's nightside.

(870 kg), spare equipment (4180 kg), and the crew itself (560 kg). These total to m_A=9820 kg.

A15: the docking/airlock/centrifuge module (DAC) mass-to-volume ratio is that of the ISS *Quest* airlock module $c_{DAC}=m_{DAC}/V_{DAC}=9923/(\pi*2^2*3)=263.216$ kg/m^3 [21].[8]

A16: the DAC is a cylinder 4 m in radius and 2 m in length accommodating a 3 m short-arm centrifuge with a total volume $V_{DAC}=\pi*4^2*2=100.531$ m^3. Although pressurized for crew access, crew time spent inside the DAC will be limited in duration because its habitable volume is shielded from radiation only by DAC structure.

A17: the DAC has mass $m_{DAC}=263.216*100.531=26{,}461$ kg (per A15 and A16).

A18: the 3 m short-arm centrifuge has mass m_C=1700 kg.[9]

A19: the minimum safe perigee height for targeting Oberth burns at Earth is +400 km.

A20: the minimum safe periapsis height for targeting Oberth burns at Mars is +384.1 km.

A21: the minimum safe pericynthion height for targeting Oberth burns at the Moon is +100 km.

A22: capacity of *Aquarius* to stow component masses is sized to the most demanding transit documented in Section 3 for each. Thus, maximum m_{RCS} (per A06) and m_P capacity are computed based on a transit with the maximum tally of change-in-velocity magnitudes $\Delta v'$. This case may differ from the transit associated with $\Delta t'$ on which maximum m_{LS} capacity is based (per A13). The m_S allocation is based on $\Delta v_D'$, the maximum tally of change-in-velocity magnitudes during departure among all transits documented in Section 3 (per A03). Each of these stowage capacity allocations is computed by applying a 1.05 inflation factor to the pertinent transit parameter.

A23: regardless of transit-specific Δv and Δt, *Aquarius* will always be loaded to capacity stowage (per A22) before an interplanetary departure. This strategy will typically provide the crew with additional radiation shielding and with positive consumables margins in the event of unexpected contingencies.

B01: *Aquarius* crew habitat beneath the surface of Deimos provides at least RP100 shielding mass such that crew radiation exposure rates are no greater than on Earth's surface. This habitat will also provide the crew with pre-emplaced power, communications, and ECLSS systems/consumables. Crew exploration of Deimos, the inner martian moon Phobos, and Mars through pre-emplaced tele-robotics is enabled from the Deimos habitat. Ideally, the entire habitat is part of a rotating centrifuge capable of

---

[8] In order to compute *Quest* volume as a single cylinder, [21] length is reduced from 5.5 m to 3 m. This is because [21]'s 4.0 m width only applies to *Quest*'s Equipment Lock. *Quest* is actually two cylinders with its Crew Lock having a much smaller width than 4.0 m.

[9] Personal communication with Jim Kukla, VP, Wyle Technology, Science and Engineering Group on 29 January 2014. This value is for an Earth-based centrifuge, and a similar 3 m unit aboard *Aquarius* would be less massive.

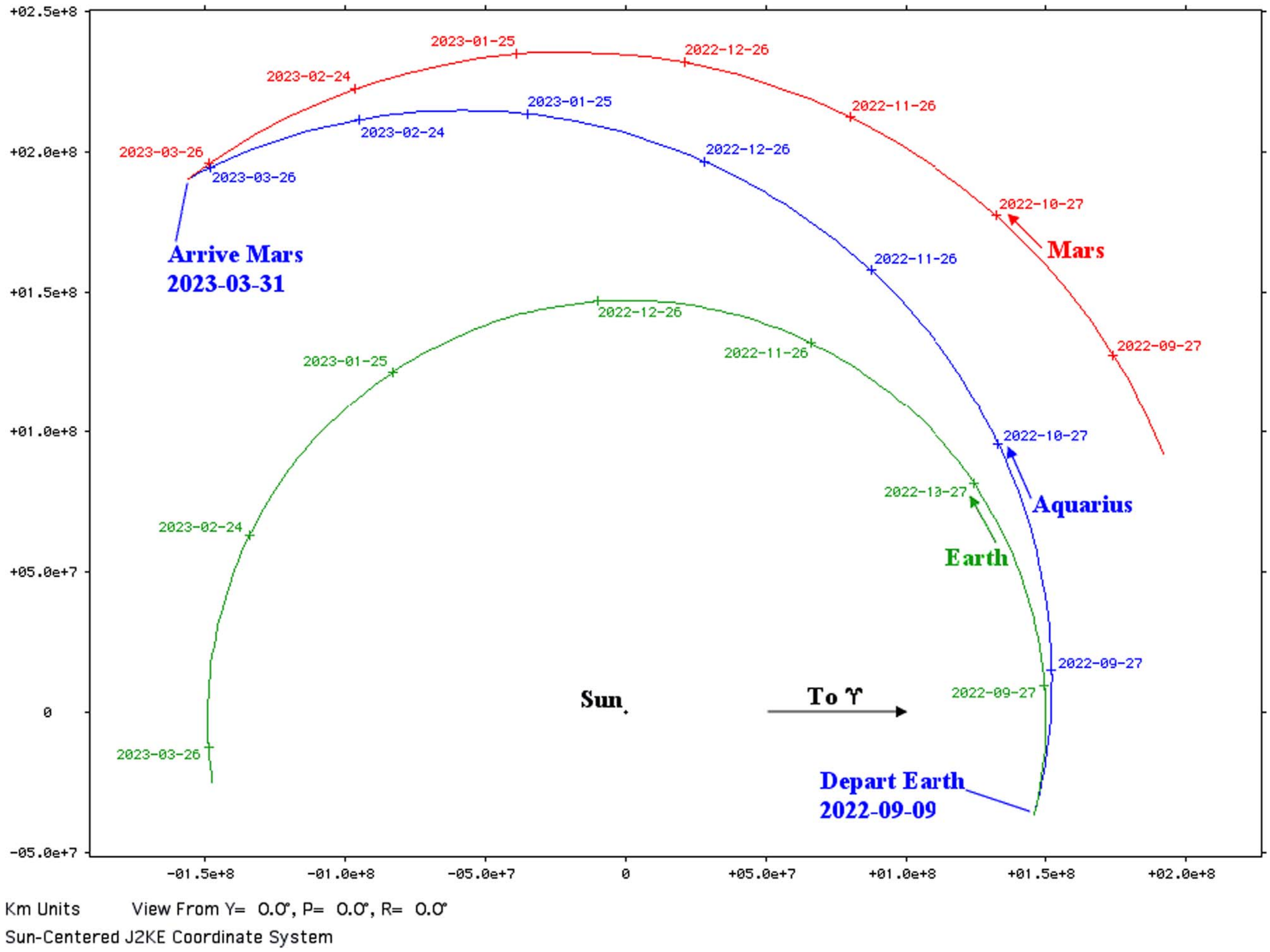

Fig. 4. *Aquarius* heliocentric motion during her maiden short-way Transit 1 is plotted (blue) along with that of Earth (green) and Mars (red) during this interval. The plot plane coincides with the ecliptic, Earth's heliocentric orbit plane. Time ticks at 30-day intervals are annotated with the date in yyyy-mm-dd format. (For interpretation of the references to color in this figure legend, the reader is referred to the web version of this article.)

generating sensed acceleration up to 1*g* for the crew with subliminal Coriolis effects. This ideal habitat may evolve after Transit 1, but a short-arm centrifuge similar to that in the DAC is assumed to be the minimal crew conditioning capability in the Deimos habitat.

B02: *Aquarius* crew habitat at SDRO-resident infrastructure will provide at least RP5 radiation shielding using structure and water masses similar to that for the Hab during *Aquarius* transits. This habitat will also provide ECLSS systems/consumables and conditioning equipment enabling the crew to attain readiness for Earth return at an atmospheric entry speed of at least 11.0 km/s within 30 days of arrival at SDRO infrastructure.

B03: during *Aquarius* assembly in EEPO, perigee height is maintained near +7700 km, reducing human and electronics exposure to particle radiation trapped in the geomagnetic field [22]. Apogee height is maintained near +113,300 km such that rendezvous phase repetition recurs each orbit, every two days. With nearly constant rendezvous phase at each EEPO launch opportunity, logistics supporting *Aquarius* assembly (per B04) are standardized.

B04: logistics supporting *Aquarius* assembly are conducted with multiple launches, each delivering a total mass of 130 t into a circular orbit at +185 km height at 45.6° inclination to Earth's equator.[10] The propellant mass fraction of this initial mass to low Earth orbit (IMLEO) is 51.4% or 66,854 kg, and that propellant delivers I_{SP}=450 s when burned to achieve rendezvous with the nascent *Aquarius* in EEPO (per B03). Immediately after rendezvous, the remaining 720 kg of this propellant mass is burned to deorbit and dispose of upper stage propulsive systems, structure, and avionics not supporting *Aquarius* assembly as payload mass.[11] In this manner, each launch delivers a payload mass of 50,360 kg, including proximity operations consumables mass in addition to that ultimately placed aboard *Aquarius*. In practice, each launch is therefore assumed to deliver 50,000 kg to *Aquarius* as she is assembled and supplied in EEPO.

B05: infrastructure supporting *Aquarius* servicing/resupply at Deimos is in proximity to the B01 habitat. Resupply water would presumably come from Earth or as an ISRU product (from Deimos or from asteroid material redirected to the vicinity of Deimos infrastructure). With an orbit period of 1.263 days, Deimos ensures periapsis at Mars flyby can be properly placed to arrive from or return to Earth on virtually any day (per A02).

B06: infrastructure supporting *Aquarius* servicing/resupply orbits the Moon with the B02 habitat in a stable, near circular SDRO whose mean radius r_0 is near 12,500 km. Resupply water would presumably come from Earth or as an ISRU product (from the

[10] This is near the minimum possible inclination for Earth departure to Mars in Transit 1. Significantly lower inclinations would be possible for another *Aquarius* maiden interplanetary transit.

[11] It should be noted that all 66,854 kg of IMLEO propellant for rendezvous and deorbit is consumed within about a day following launch. Consistent with I_{SP} = 450 s, this propellant is therefore assumed to be cryogenic with minimal concern for significant thermal losses, thanks to its prompt consumption.

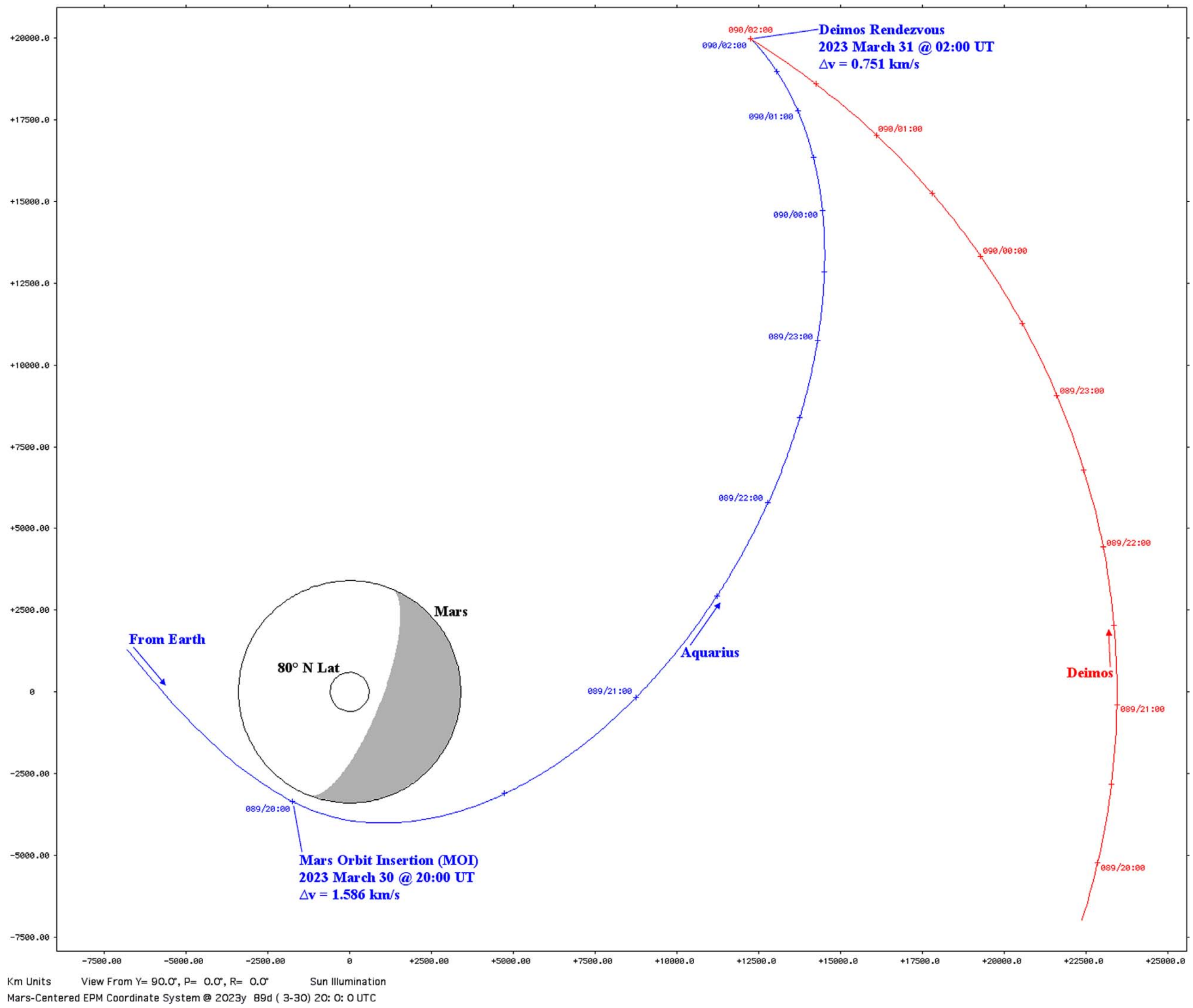

Fig. 5. Mars-centered inertial *Aquarius* motion (blue) is plotted during her first rendezvous with Deimos (red). The plot plane coincides with that of the martian equator. Time tick labels are 2023 March 30-31 UT in DOY/hh:mm format. The shaded area is the nightside of Mars. This shading indicates *Aquarius* approaches Deimos with at least half of the moon's lit surface visible. (For interpretation of the references to color in this figure legend, the reader is referred to the web version of this article.)

Table 2
Transit 2 burns are summarized as *Aquarius* departs Deimos and arrives at Earth and SDRO-resident infrastructure. The leftmost column provides the date and universal time (UT) of each event in the rightmost column. Values in the Δv column are positive for prograde burns and negative for retrograde burns. A total $\Delta v = 3.827$ km/s is expended over $\Delta t = 240$ days during Transit 2 with $\Delta v_D = 2.205$ km/s.

Date @ UT	Δv (km/s)	Event
2024 Aug 08 @ 17:30	−0.652	Depart Deimos for Mars flyby
2024 Aug 09 @ 00:00	+1.553	Trans-Earth injection (TEI)
2025 Apr 03 @ 00:00	−0.935	Trans-lunar injection (TLI)
2025 Apr 05 @ 21:44	−0.378	Lunar orbit insertion (LOI)
2025 Apr 06 @ 05:19	+0.309	SDRO-resident infrastructure rendezvous

Moon and asteroids redirected to SDRO). With $r_0 >> 3000$ km, infrastructure trajectory perturbations from local variations in lunar gravity need not be periodically corrected to avoid impact on the Moon. With $r_0 << 70{,}000$ km, gravity perturbations from the Earth and Sun leading to orbit instability are also avoided. At $r_0 = 12{,}500$ km, selenographic period (equivalent to the interval cycling through all phase angles with respect to the Earth/Moon line) is a moderate 1.38 days. Consequently, optimal phase for arriving at or departing from SDRO infrastructure can be achieved in a few lunar orbits with semi-major axis differing from 12,500 km (and pericynthion height above +100 km, per A21) or by varying transit time between the Earth and Moon. At 27.3 days, the Moon's geocentric orbit period is just short enough to ensure perigee at Earth flyby can be properly placed to depart for or return from Deimos during the interval *Aquarius* capabilities support an interplanetary transit (per A02).

3. The first three interplanetary transits by *Aquarius*

The first three subsections to follow document each of the first three transits to be made by *Aquarius* after her assembly in EEPO (per B03 and B04). None of these transits pertain to robotic cargo logistics supporting habitats and *Aquarius* resupply at Deimos or in SDRO, which are beyond the scope of this paper. A fourth subsection contains notes on unique or comparative aspects of these transits' trajectory designs. Transit 1, the maiden voyage of *Aquarius*, departs EEPO in late 2022 such that Mars is near aphelion when *Aquarius* arrives for Deimos rendezvous. This transit is near the start of a sequence of high Δv Mars mission opportunities

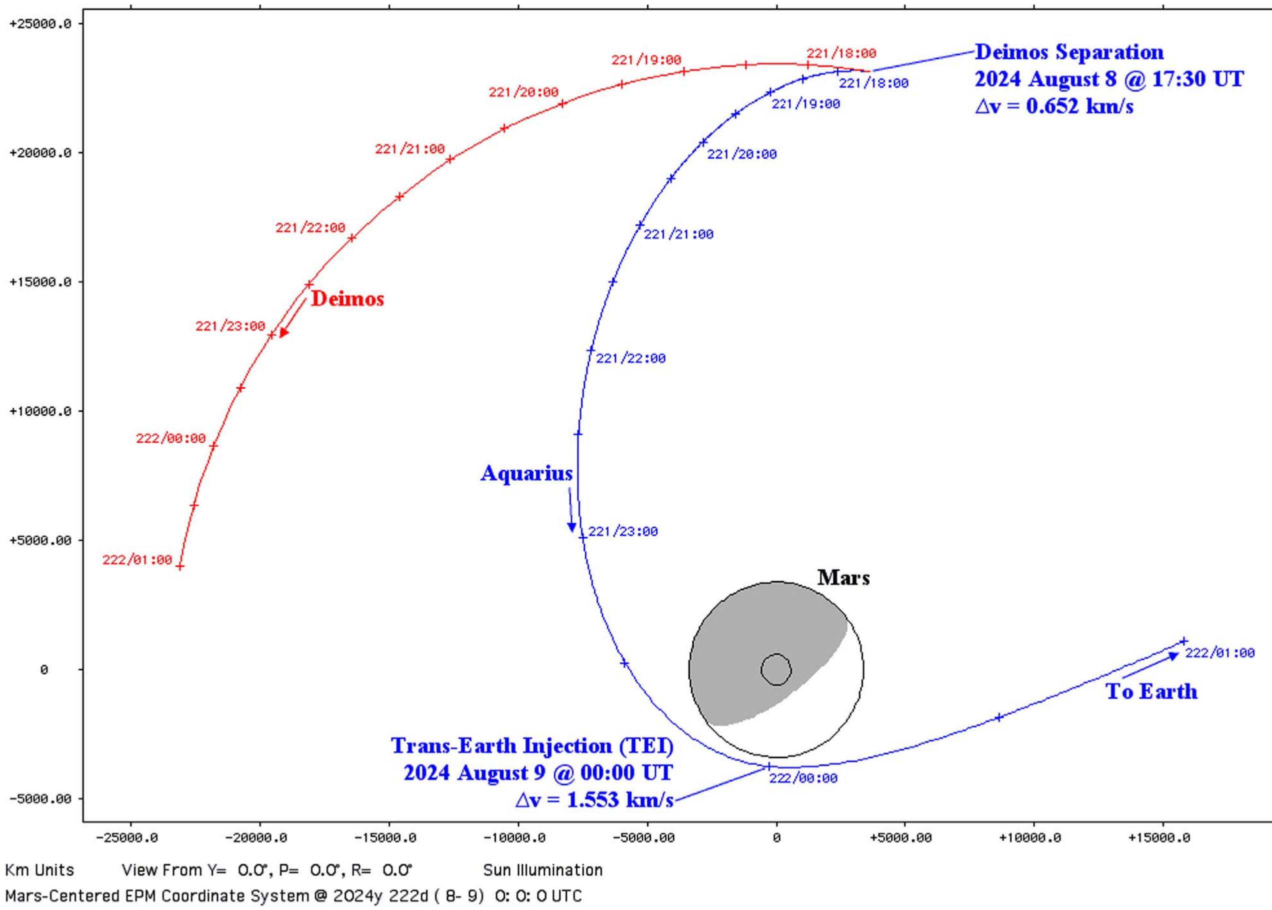

Fig. 6. Mars-centered inertial *Aquarius* motion (blue) is plotted during her first departure from Deimos (red). The plot plane coincides with that of the martian equator. Time tick labels are 2024 August 8-9 UT in DOY/hh:mm format. The shaded area is the nightside of Mars. This shading indicates *Aquarius* departs Deimos with at least half of the moon's lit surface visible. (For interpretation of the references to color in this figure legend, the reader is referred to the web version of this article.)

from Earth ([11], p. 5) and is timed with the intent of stressing *Aquarius* capabilities to the degree they cover any conjunction class mission opportunity to Deimos (per A01 and A02). Although proving this to be the case universally is beyond the scope of this paper, *Aquarius* Δv capability will cover the challenging transits documented here to margins of approximately +5% or more (per A22). A timeline spanning Transits 1, 2, and 3 appears in Fig. 1.

Trajectory designs for Transits 1–3 are manually optimized for minimal Δv tallies among all burns within the arrival constraints of A04. An automated optimizer would undoubtedly improve on these designs, perhaps to a significant degree. But the objective here is to demonstrate *Aquarius* can fly practical trajectories, even when interplanetary geometry is uncooperative. To that end, fully optimizing transit cases documented in this section could suggest *Aquarius* capabilities insufficient to cover worse cases not yet studied.

Although some trajectory design parameters such as v_∞ inherently reflect a patched conic pedigree, data presented in this section represent preliminary segmented transits as evolved into continuous precision trajectories. The only discontinuities remaining following this evolution are velocity increments associated with impulsively approximated NTP burns. Precision trajectories are numerically integrated [23] and simulate gravity accelerations from the Sun, Earth, Mars, and Moon along with excess equatorial mass within the oblate figures of Earth and Mars. Ephemerides for the Earth, Mars, and Moon as documented in [24], Appendix II are utilized throughout this section. Mars-centered Deimos positions are from the Jet Propulsion Laboratory's *Horizons* computation service [25].

A trajectory design feature common to all transit termini, whether departing EEPO, departing/arriving Deimos, or departing/arriving SDRO, is the Oberth maneuver. At each terminus, distance from the Earth/Mars/Moon is sufficiently great, along with departure/arrival v_∞, to warrant this technique. Under these conditions, minimal Δv required to depart/arrive a terminus is obtained when the required prograde/retrograde burn is performed as close to the Earth/Mars/Moon as safety permits. This precept holds in Transits 1–3 even though a second retrograde/prograde burn at each terminus must be paired with the opposing prograde/retrograde burn close to the Earth/Mars/Moon.

As an example, consider departure from or arrival at Deimos. The Direct strategy for departure/arrival entails a single prograde/retrograde burn to/from a Mars-centered hyperbola whose periapsis height is exactly that of Deimos (+20,073.3 km in this example). In contrast, the Oberth strategy utilizes two burns. For departure, a retrograde burn at Deimos initiates a Hohmann transfer to Mars periapsis height +384.1 km (per A20), where a prograde burn imparts escape from Mars. For arrival, Mars capture from the approach hyperbola is achieved with a retrograde burn at the +384.1 km periapsis height, initiating Hohmann transfer to Deimos, where a prograde burn achieves rendezvous at Mars apoapsis.

Total impulsive Δv values[12] for the Direct and Oberth strategies

[12] In the interest of simplicity, these values assume the Mars depart/approach asymptote lies in the Deimos orbit plane such that out-of-plane burn components are absent. Transits 1–3 do possess these burn components, but the associated plane changes would challenge both the Direct and Oberth strategies equally. A four-burn "bi-elliptic" arrival or departure can often significantly reduce Δv with

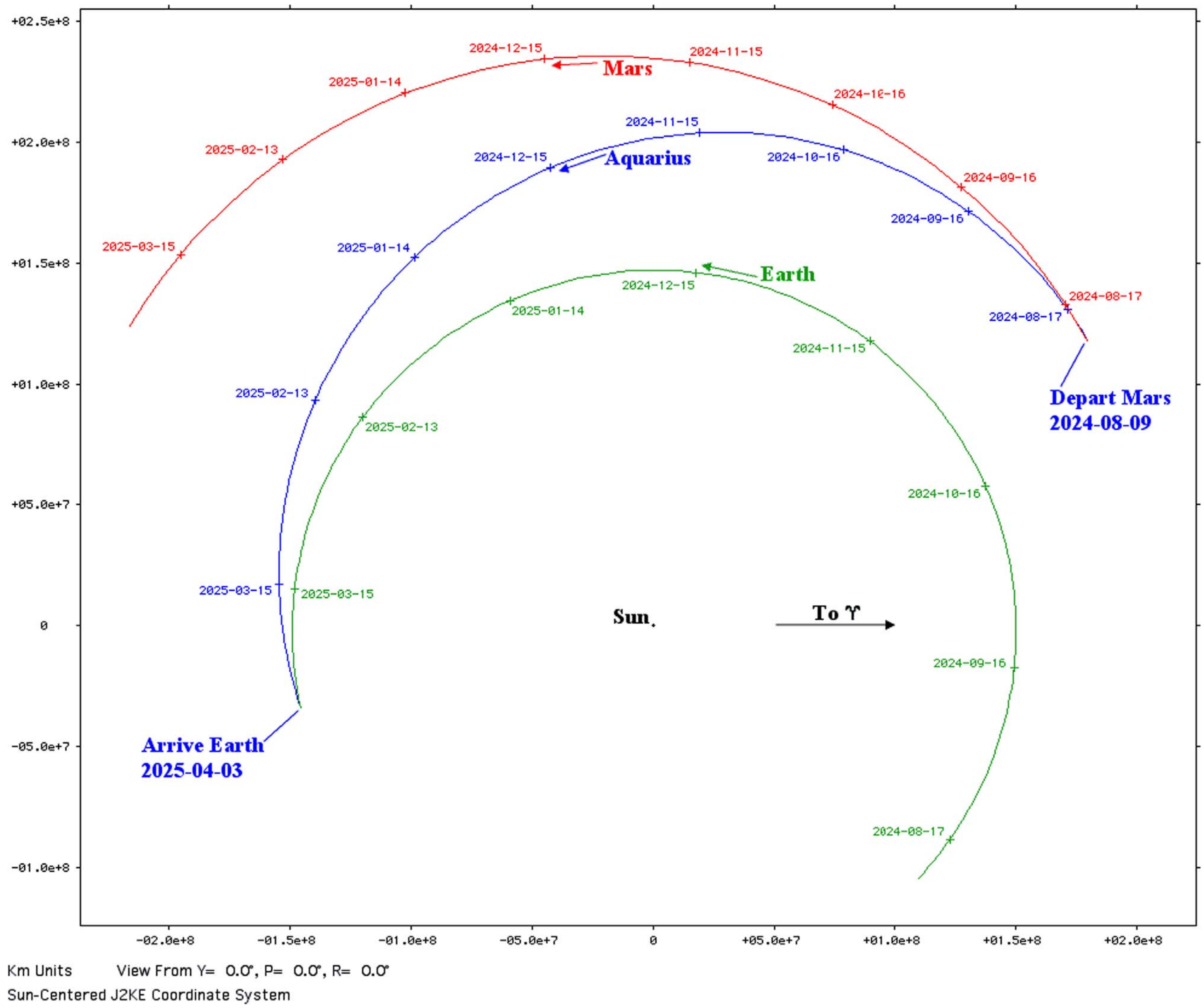

Fig. 7. *Aquarius* heliocentric motion during her short-way Transit 2 is plotted (blue) along with that of Earth (green) and Mars (red) during this interval. The plot plane coincides with the ecliptic, Earth's heliocentric orbit plane. Time ticks at 30-day intervals are annotated with the date in yyyy-mm-dd format. (For interpretation of the references to color in this figure legend, the reader is referred to the web version of this article.)

are plotted as functions of Mars depart/arrive v_∞ in Fig. 2. These plots indicate Deimos arrival/departure with $v_\infty > 2.0$ km/s requires less Δv using the two-burn Oberth strategy than would a single Direct strategy burn. Such is clearly the case for all transits documented here. The Transit 1 Deimos arrival has $v_\infty = 3.658$ km/s, Transit 2 Deimos departure has $v_\infty = 3.471$ km/s, and Transit 3 Deimos arrival has $v_\infty = 4.215$ km/s.

3.1. Transit 1: EEPO to Deimos

The maiden interplanetary transit of *Aquarius* begins by utilizing the Oberth strategy to depart her assembly EEPO and escape Earth on an interplanetary trajectory intercepting Mars. A similar strategy is employed at the transit's arrival terminus to achieve Mars capture and rendezvous with Deimos. The transit's burns are summarized in Table 1.

Fig. 3 plots inertial geocentric motion of *Aquarius* from her final EEPO through perigee lowering and TMI burns. Note perigee lowering also serves as an NTP systems test before committing *Aquarius* to interplanetary space post-TMI. Fig. 4 plots heliocentric motion of Earth, Mars, and *Aquarius* during Transit 1, while Fig. 5 plots Mars-centered Deimos and *Aquarius* motion as Transit 1 concludes.

Upon arrival at Deimos, *Aquarius* crew transfer to the pre-emplaced RP100 subsurface habitat is expedited to minimize radiation exposure (per A04 and B01). Ideally, this transfer would be facilitated by a pressurized docking interface. Such an interface would also simplify transfer of pre-emplaced water and other consumables from Deimos infrastructure to *Aquarius* in preparation for Transit 2 (per B05). In addition to Transit 2 preparations, the 496-day Deimos loiter interval following Transit 1 would be filled with Deimos and Mars exploration activities in which the *Aquarius* crew operates pre-emplaced tele-robotic systems from its subsurface habitat (per B01).

3.2. Transit 2: Deimos to SDRO

The second interplanetary transit of *Aquarius* begins by utilizing the Oberth strategy to depart Deimos and escape Mars on an interplanetary trajectory intercepting Earth. This strategy is

(*footnote continued*)
respect to Direct or Oberth when out-of-plane motion is present, but this strategy is considered over-optimization that could lead to insufficient *Aquarius* performance margins as previously documented in this section. Furthermore, bi-elliptic arrivals will typically introduce undesirable delays to crew Deimos/SDRO habitat access, likely in violation of A03.

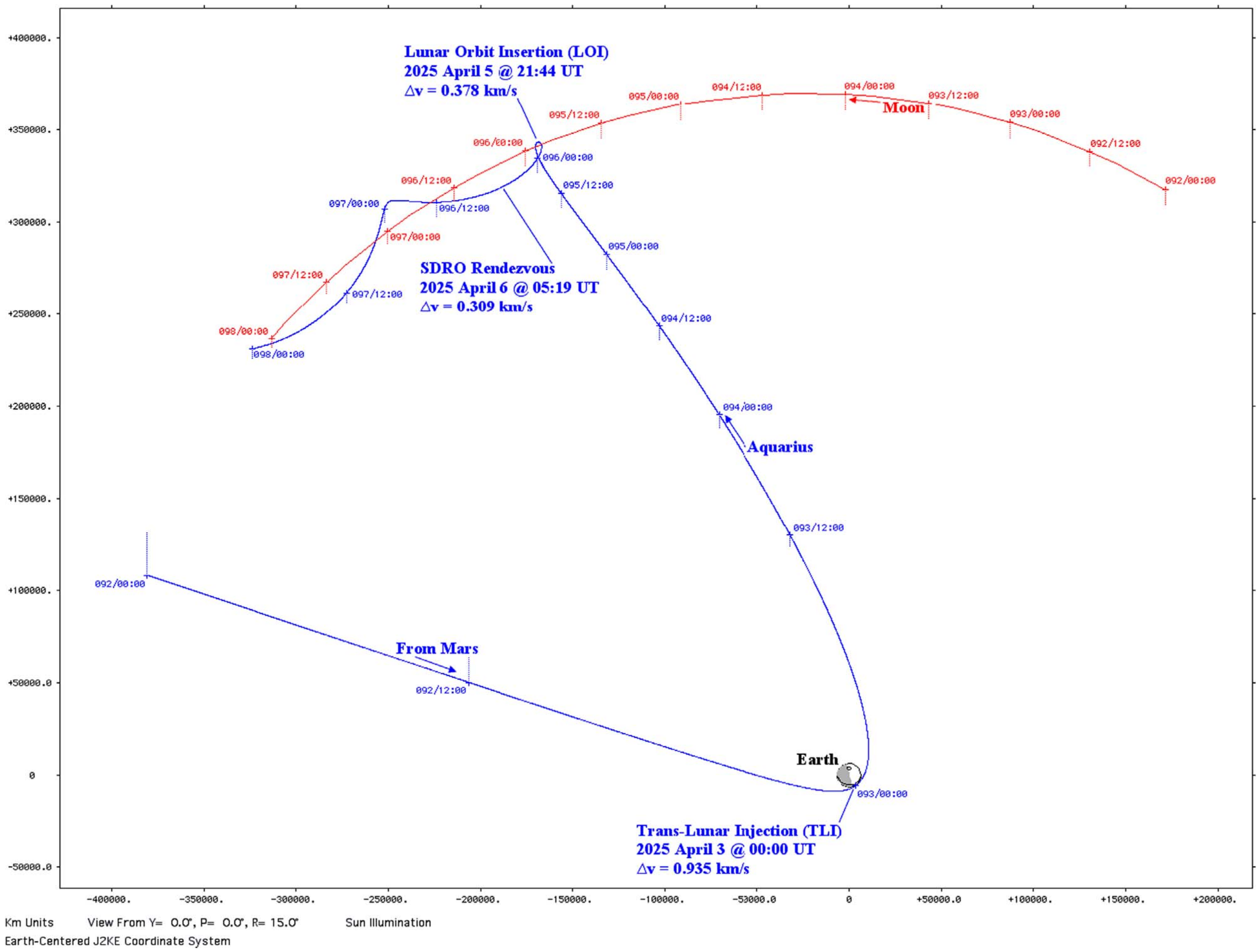

Fig. 8. Geocentric inertial motion of *Aquarius* (blue) and the Moon (red) are plotted as the spacecraft returns to her SDRO "garage" for the first time. The plot plane nearly coincides with the plane of *Aquarius* motion. Time tick labels are 2025 April 2-8 UT in day-of-year (DOY)/hh:mm format. Dotted lines are projections onto the ecliptic plane, and the shaded area is Earth's nightside. From this shading, note how the Moon must be slightly past first quarter phase at LOI to minimize TLI Δv. (For interpretation of the references to color in this figure legend, the reader is referred to the web version of this article.)

employed twice upon Earth arrival. The first instance achieves Earth capture and initiates lunar intercept when *Aquarius* performs her first trans-lunar injection (TLI) burn, and the second achieves lunar capture followed by rendezvous with SDRO-resident infrastructure. Transit 2′s burns are summarized in Table 2.

Fig. 6 plots inertial Mars-centered motion of *Aquarius* and Deimos from Deimos separation through the TEI burn. Fig. 7 plots heliocentric motion of Earth, Mars, and *Aquarius* during Transit 2, while Fig. 8 plots geocentric Moon and *Aquarius* motion as Transit 2 concludes. Fig. 9 plots selenocentric motion as *Aquarius* reaches the Moon and achieves rendezvous with SDRO-resident infrastructure at $r_0 = 12{,}500$ km.

Upon docking with SDRO-resident infrastructure, *Aquarius* crew transfer to RP5 habitat is expedited to minimize radiation exposure (per A04 and B02). Ideally, this transfer would be facilitated by a pressurized docking interface. Such an interface would also simplify transfer of pre-emplaced water and other consumables from the SDRO infrastructure to *Aquarius* in preparation for Transit 3 (per B06).

3.3. Transit 3: SDRO to Deimos

As illustrated by Fig. 9, the initial rendezvous performed by *Aquarius* with SDRO-resident infrastructure at the conclusion of Transit 2 assumes that infrastructure has cooperatively phased to the optimal SDRO position just as *Aquarius* reaches her first post-LOI apocynthion nearby. Absent such cooperative phasing, *Aquarius* would under-burn the Transit 2 LOI to enter a more eccentric intermediate phasing orbit (with apocynthion exceeding the SDRO's $r_0 = 12{,}500$ km) before completing the Transit 2 LOI and achieving rendezvous. Although *Aquarius* active phasing with SDRO infrastructure would have little impact on Transit 2 total Δv, her crew would be exposed to additional radiation in the Hab with RP < 5 during time spent in the phasing orbit. This tends to conflict with A03.

Such a conflict does not develop when departing SDRO infrastructure to initiate Transit 3. With a full consumables load, *Aquarius* provides considerably more than RP5 Hab shielding at this time. Initial conditions for Transit 3 therefore assume the Fig. 9 SDRO is coasted 574 days (398 orbits, as reckoned by tallying ascending node crossings on the lunar equator) into the next Earth departure season for Mars. To depart the SDRO and lunar orbit for Earth and TMI at the beginning of Transit 3 then requires *Aquarius* perform TEI in three parts. A retrograde TEIa burn enters a phasing orbit with pericynthion height near +4936 km, a retrograde TEIb burn lowers pericynthion height to +100 km two orbits after TEIa, and a prograde TEIc burn departs the Moon for Earth. Thanks to the TEIa and TEIb burns, TEIc can be performed at the selenocentric position and time required for a near-Earth TMI in fulfillment of Transit 3 Oberth departure strategy. These initial burns and those required to achieve Transit 3 Deimos rendezvous appear in Table 3.

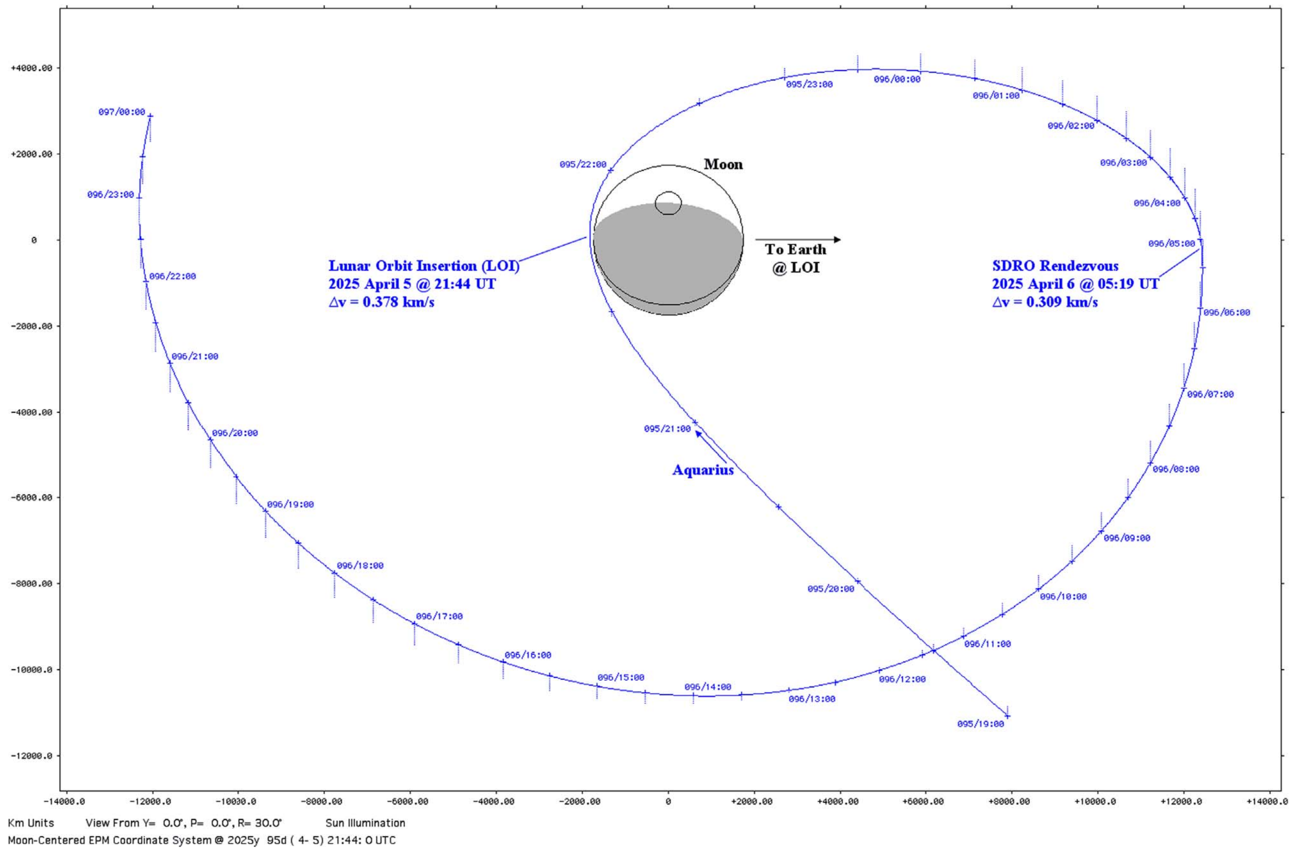

Fig. 9. Selenocentric inertial motion of *Aquarius* is plotted as she achieves capture in the lunar gravity field and conducts rendezvous with SDRO-resident infrastructure at r_0=12,500 km. The plot plane nearly coincides with the plane of *Aquarius* motion. Time tick labels are 2025 April 5-7 UT in day-of-year (DOY)/hh:mm format. Dotted lines are projections onto the lunar equatorial plane, and the shaded area is the Moon's nightside.

Fig. 10 plots selenocentric *Aquarius* motion as she departs SDRO-resident infrastructure and leaves the Moon for Earth while performing the TEIa, TEIb, and TEIc burns. Effects from this burn sequence, together with TMI, are plotted geocentrically for *Aquarius* accompanied by the Moon's motion in Fig. 11. Heliocentric motion of Earth, Mars, and *Aquarius* during Transit 3 are plotted in Fig. 12. Finally, Mars-centered motion of Deimos and *Aquarius* are plotted in Fig. 13 as Transit 3 is completed.

3.4. Trajectory design notes

Among conceivable *Aquarius* transit departures or arrivals, initial EEPO departure is unique because no previous constraint conflicts with precise alignment between the EEPO plane and that of the associated Earth departure hyperbola. Other transports might manage planar misalignment between the terminus orbit and the departure/approach hyperbola by adding a dedicated plane change burn to the Oberth strategy. Such a burn is best performed at the lowest possible speed and typically imposes an increase in Δt while a large distance from the Earth/Mars/Moon is achieved before escape in a departure or after capture in an arrival. The increased Δt associated with this "detour" is generally undesirable for human spaceflight, and it conflicts with A04 in an arrival. Consequently, Oberth burns performed by *Aquarius* contain appreciable out-of-plane Δv components, the only exception being departure from her assembly EEPO to begin Transit 1.

As noted in B05, the short orbit period of Deimos helps facilitate Oberth departures and arrivals at Mars on virtually any day. Per B06, the Moon's much longer orbit period could pose challenging constraints to Oberth departures and arrivals at Earth. These challenges are managed with tolerable Δv increases in

Table 3
Transit 3 burns are summarized as *Aquarius* departs SDRO and arrives at Deimos. The leftmost column provides the date and universal time (UT) of each event in the rightmost column. Values in the Δv column are positive for prograde burns and negative for retrograde burns. A total Δv=4.437 km/s is expended over Δt=241 days during Transit 3 with Δv_D=1.696 km/s.

Date @ UT	Δv (km/s)	Event
2026 Nov 01 @ 11:41	−0.109	TEIa lowers SDRO pericynthion height to +4936 km
2026 Nov 03 @ 09:26	−0.208	TEIb lowers pericynthion height to +100 km
2026 Nov 03 @ 16:52	+0.488	TEIc departs Moon for Earth
2026 Nov 06 @ 23:49	+0.891	TMI
2027 Jun 29 @ 15:30	−1.940	MOI
2027 Jun 29 @ 22:00	+0.801	Deimos rendezvous

Transits 2 and 3. In an Earth departure transit, it might be acceptable to depart SDRO and the Moon a few weeks before TMI to achieve the proper perigee geometry for TMI, assuming the increased Δt did not violate A13. At the end of an Earth return transit, however, a post-TLI loiter of several weeks to encounter the Moon would likely violate A03 even if compliant with A13.

Short-way heliocentric transits between Earth and Mars (per A02) are in a plane inclined to the ecliptic by at most a few degrees. The Moon's equator and geocentric orbit plane are closely aligned with the ecliptic, and this alignment facilitates departures and arrivals at SDRO, the Moon, and Earth. Although the orbit of Deimos about Mars is nearly in the martian equatorial plane, that

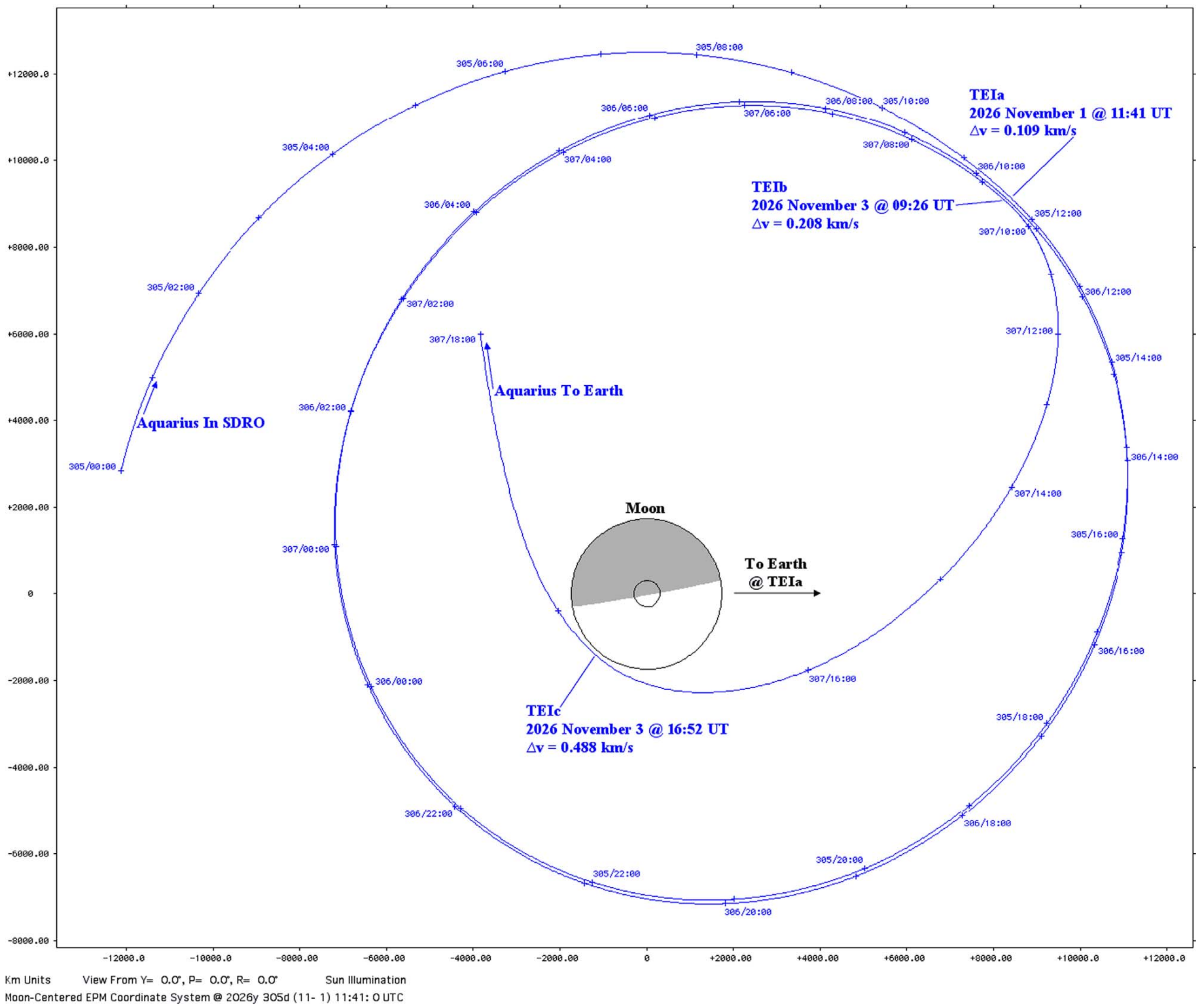

Fig. 10. Selenocentric inertial motion of *Aquarius* is plotted as she departs SDRO for Earth and TMI. The plot plane coincides with the Moon's equator and very nearly coincides with that of *Aquarius* motion. Time tick labels are 2026 November 1-3 UT in day-of-year (DOY)/hh:mm format, and the shaded area is the Moon's nightside.

plane is inclined to the ecliptic by 26.7°. It is therefore no surprise that Transit 3 approaches Mars in a trajectory plane inclined 30.0° to the martian equator and requires considerably more Δv at MOI and at Deimos rendezvous than does Transit 1, whose arrival inclination is 23.3° to the martian equator (see Tables 1 and 3 to compare Δv values in Transits 1 and 3, respectively).

4. *Aquarius* transit departure mass baseline and assessments

None of the following analysis pertains to robotic cargo logistics vehicles supporting habitats and *Aquarius* resupply at Deimos or in SDRO. At any point in time during a transit, *Aquarius* total mass is obtained from the following summation.

$$m_{TOT} = m_A + m_C + m_{DAC} + m_H + m_{LS} + m_{NTP} + m_P + m_{RCS} + m_S + m_T \quad (1)$$

Of these component masses, only m_{LS} and m_P are to be modeled as dynamic quantities during a transit (m_{RCS} would be dynamic in real world transits but is conservatively held at its transit departure value in lieu of an attitude timeline per A06). This section first develops a transit departure baseline for *Aquarius* total mass under A22 assumptions. Per A23, this baseline will apply to departure on any interplanetary transit. The baseline is then assessed against each of the transits documented in Section 3 to verify adequate NTP propellant, radiation shielding, and ECLSS consumables margins. Note that mass values reported in this section are rounded to the nearest kg from extended precision computations.

Buildup of the *Aquarius* departure mass baseline begins by computing m_{LS}'. Per A13, this quantity depends on $\Delta t'$, and a survey of captions for Tables 1–3 shows $\Delta t'$=241 days during Transit 3. Thus, m_{LS}'=1.05∗241∗98.61=24,953 kg.

Although the m_{LS}' value will be decremented with transit time T during an assessment, it will be held constant as a simplifying and conservative approximation when used in the rocket equation to obtain m_P and m_S at departure. This approximation leads to the definition of static *Aquarius* mass for use in the rocket equation.

$$m_Z = m_A + m_C + m_{DAC} + m_H + m_{LS}' + m_{NTP} \quad (2)$$

Therefore, m_Z=9820 (per A14)+1700 (per A18)+26,461 (per A17)+36,457 (per A11)+24,953 (per A13)+41,700 (per A05)=141,091 kg.

Another survey of captions for Tables 1–3 shows $\Delta v'$=4.437 km/s during Transit 3 and $\Delta v_D'$=2.205 km/s during Transit

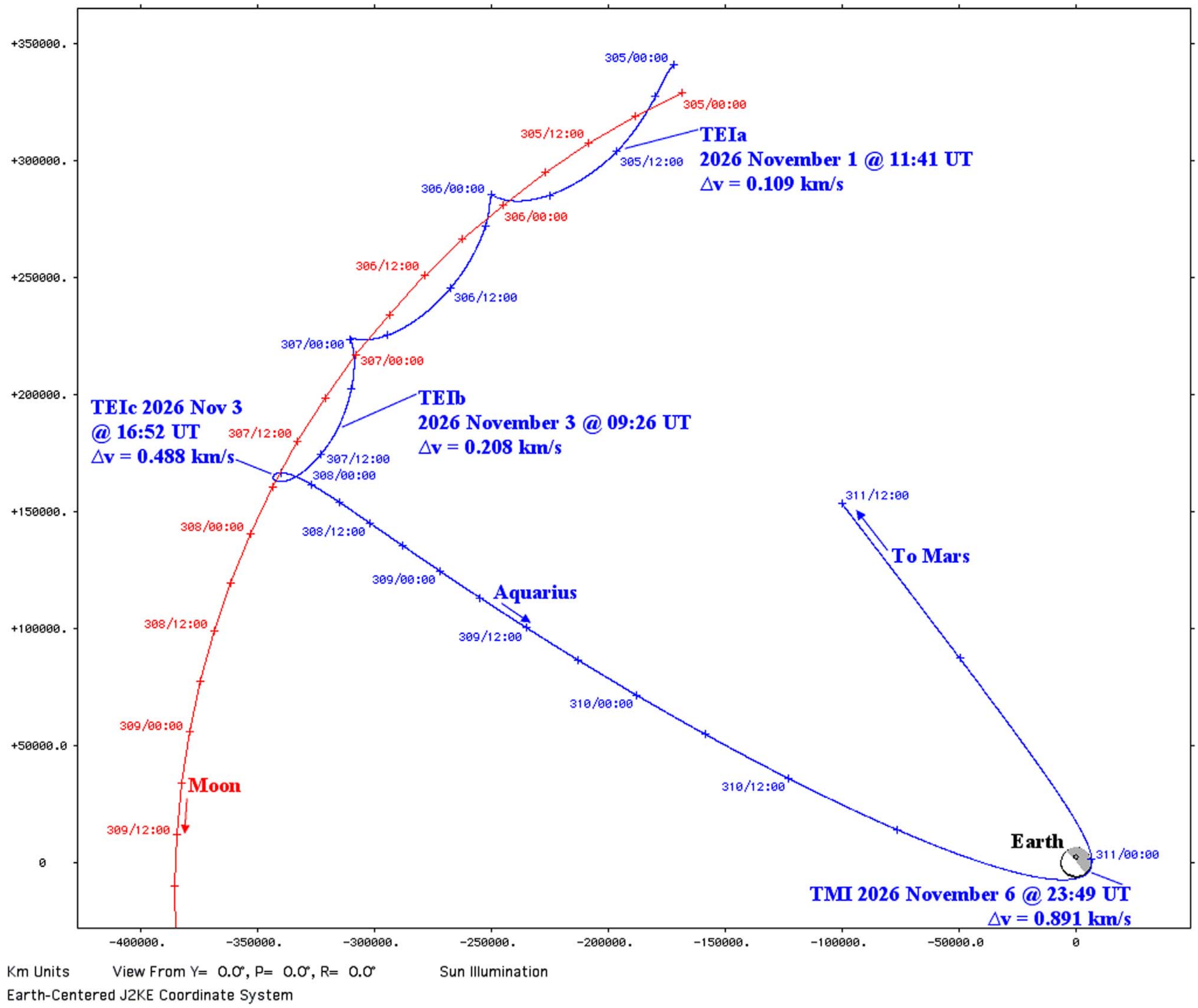

Fig. 11. Geocentric inertial motion of the Moon (red) and *Aquarius* (blue) are plotted as SDRO and Earth are departed for Mars. The plot plane coincides with the ecliptic plane and very nearly that of *Aquarius* motion. Time tick labels are 2026 November 1-7 UT in day-of-year (DOY)/hh:mm format, and the shaded area is Earth's nightside. From this shading, note how the Moon must be slightly past last quarter phase at TEIc to minimize TMI Δv. (For interpretation of the references to color in this figure legend, the reader is referred to the web version of this article.)

2. The rocket equation for all of Transit 3 is then expressed as follows, substituting $m_{RCS}=c_{RCS}\,(m_P+m_S)$ per A06 and $m_T=c_T\,(m_P+m_S)$ per A07. In the natural exponent (exp) argument, note $\Delta v'$ has been amplified by 5% per A22.

$$m_Z + m_P + c_{RCS}(m_P + m_S) + m_S + c_T(m_P + m_S) = \left[m_Z + c_{RCS}(m_P + m_S) + m_S + c_T(m_P + m_S)\right]\exp\{1.05\,\Delta v'/v_X\} \quad (3)$$

The rocket equation for Transit 2's Deimos/Mars departure is expressed in a manner similar to that for Transit 3, where the m_J constraint is valued per A12.

$$m_Z + m_P + c_{RCS}(m_P + m_S) + m_S + c_T(m_P + m_S) = \left[m_Z + c_{RCS}(m_P + m_S) + m_J + c_T(m_P + m_S)\right]\exp\{1.05\,\Delta v_D'/v_X\} \quad (4)$$

Exponential factors in (Eqs. (3) and 4) are abbreviated as $A=\exp\{1.05\ \Delta v'/v_X\}$ and $B=\exp\{1.05\ \Delta v_D'/v_X\}$, respectively. This notation is used in the following expressions for m_P and m_S resulting from simultaneous solution of (Eqs. (3) and 4).

$$m_P = \frac{(1 - A)B\left(m_Z + m_J\{c_{RCS} + c_T + 1\}\right)}{A\left(\{c_{RCS} + c_T\}\{B - 1\} - 1\right)} \quad (5)$$

$$m_S = \frac{A\left(m_Z + m_J\{c_{RCS} + c_T\}B\right) - B\left(m_Z + m_J\{c_{RCS} + c_T + 1\}\right)}{A\left(\{c_{RCS} + c_T\}\{B - 1\} - 1\right)} \quad (6)$$

With this simultaneous solution, the transit departure baseline for *Aquarius* total mass can be computed per A22. Table 4 provides the mass for each Eq. (1) component of this baseline.

Per A13, m_{LS} is 3∗29.26/98.61=89.017% water by mass. Using Table 4 values, *Aquarius* is therefore $(0.89017m_{LS}+m_P+m_S)/m_{TOT}$=53.7% water by mass at an interplanetary departure. She is truly The Water-Bearer.

Per B04 and Table 4's value for m_{TOT}, 356,819/50,000=7.14 launches are required to assemble *Aquarius* in EEPO and supply her there for a maiden transit to Deimos. Except for m_P, which will require nearly 3 launches for delivery, no single Table 4 *Aquarius* mass component exceeds the deliverable payload capacity of 50,000 kg per launch. A smaller crew ferry launch vehicle with

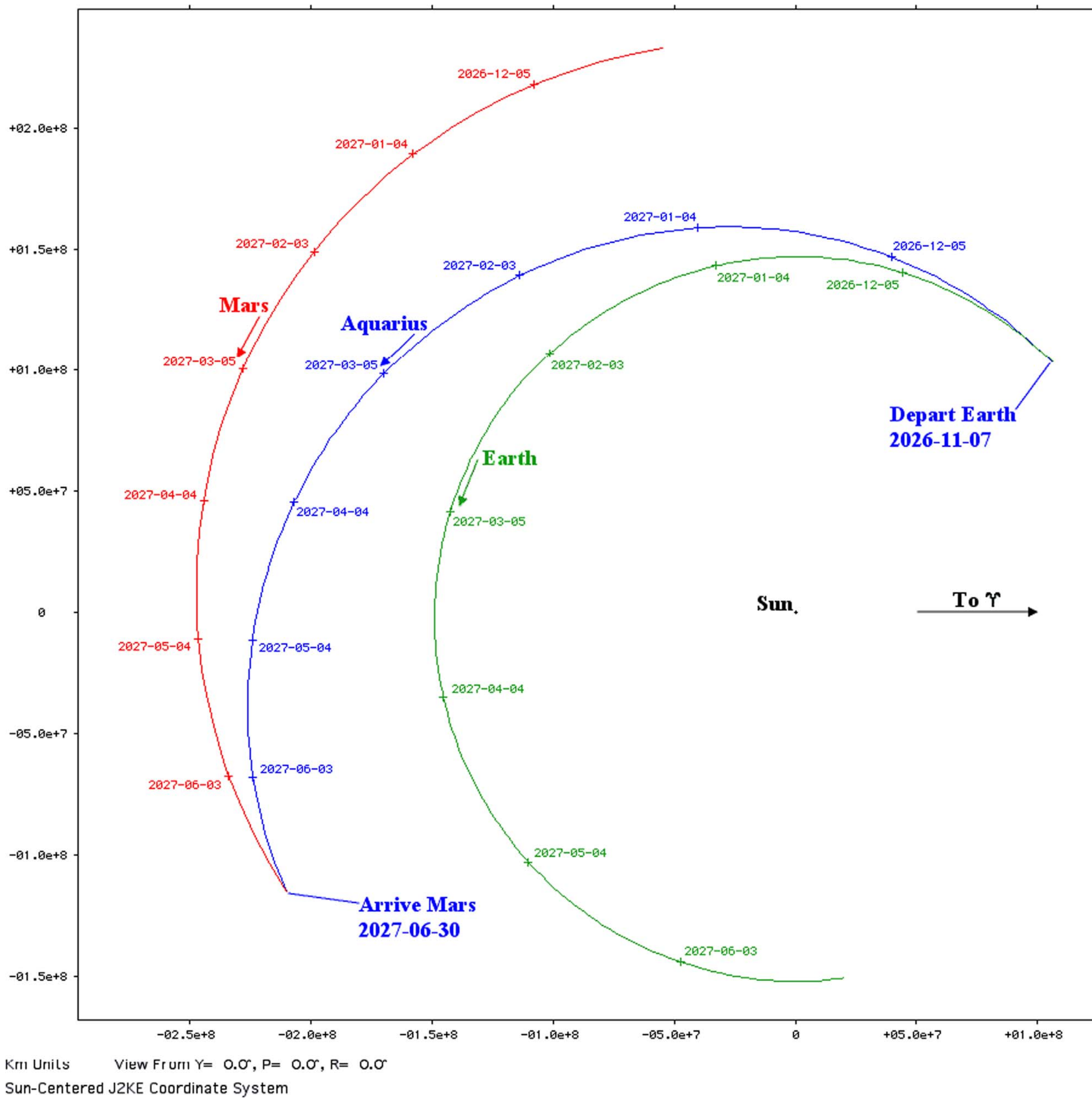

Fig. 12. *Aquarius* heliocentric motion during her short-way Transit 3 is plotted (blue) along with that of Earth (green) and Mars (red) during this interval. The plot plane coincides with the ecliptic, Earth's heliocentric orbit plane. Time ticks at 30-day intervals are annotated with the date in yyyy-mm-dd format. (For interpretation of the references to color in this figure legend, the reader is referred to the web version of this article.)

considerably less than 130 t IMLEO performance could supply the fractional payload mass requiring an eighth launch. In this manner, the crew, their gear, and sundry personal items would presumably be the final delivery to *Aquarius* in EEPO.

Tables 5–7 summarize depletion of the Table 4 departure baseline during Transits 1–3, respectively. These baseline assessments indicate margins per A03, A13, A22, and A23 are adequate during each of the transits documented in Section 3.

Of all the NTP burns documented in Tables 5–7 during planetary departure, Transit 2's TEI has the largest propellant consumption, amounting to 120,934 − 67,462 = 53,472 kg according to the m_P column in Table 6. Because m_{TOT} is nearly at its fully loaded value immediately before TEI, this burn is near the greatest duration *Aquarius* is likely to encounter during nominal short-way transits between Earth and Mars. Effective water flow rate during an NTP burn is F/v_X = 333,617/8826 = 37.8 kg/s (per A05).[13] The TEI burn is therefore 53,472/37.8 = 1415 s = 23.6 min in duration.

Table 7 shows the slimmest margin with respect to m_{LS} for Transits 1–3 to be +1188 kg, as expected. The consumption rate required to bring m_{LS} to zero at the end of Transit 3 would be $m_{LS}'/\Delta t$ = 24,953/241 = 103.54 kg/day. With respect to A13's assumed consumption rate, the zero margin rate is greater by a factor of 103.54/96.61 = 1.05 per A13.

Table 7 also shows the slimmest m_P margin for Transits 1–3 at arrival to be +11,757 kg, as expected. Total *Aquarius* propulsive

[13] The flow rate computation must use exhaust speed units of m/s in order to be compatible with thrust units of Nt, equivalent to kg-m/s^2.

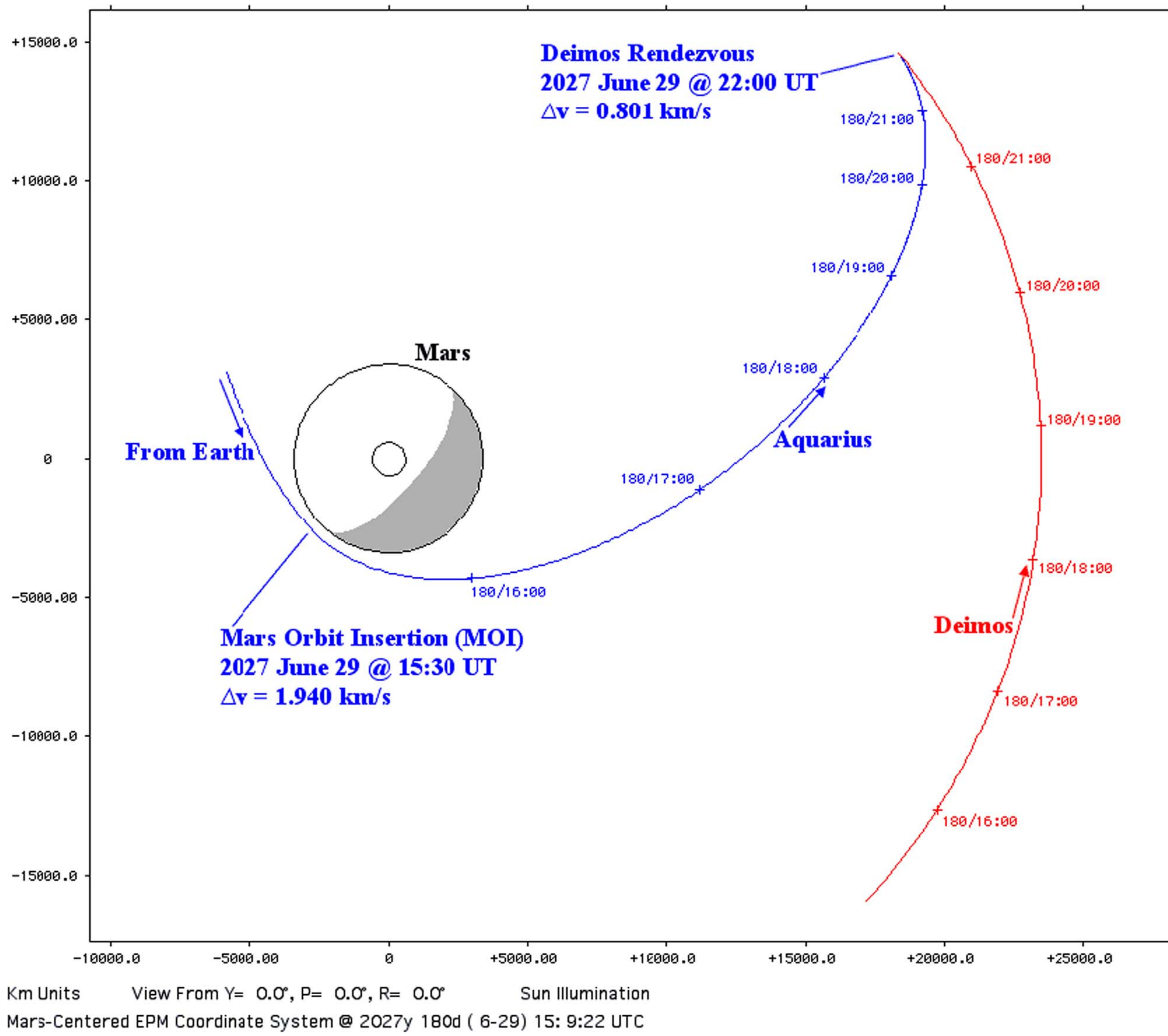

Fig. 13. Mars-centered inertial *Aquarius* motion (blue) is plotted during her second rendezvous with Deimos (red). The plot plane coincides with that of the martian equator. Time tick labels are 2027 June 29 UT in DOY/hh:mm format. The shaded area is the nightside of Mars. This shading indicates *Aquarius* approaches Deimos with at least half of the moon's lit surface visible. (For interpretation of the references to color in this figure legend, the reader is referred to the web version of this article.)

Table 4
The *Aquarius* departure mass baseline is summarized with values for each component of Eq. (1), ending with the components' sum, m_{TOT}.

Component	Reference	Mass (kg)
m_A	A14	9820
m_C	A18	1700
m_{DAC}	A17	26,461
m_H	A11	36,457
m_{LS}	A13, Transit 3 $\Delta t'$=241 days	24,953
m_{NTP}	A05	41,700
m_P	Eq. (5), Transit 3 $\Delta v'$=4.437 km/s	146,343
m_{RCS}	A06	13,903
m_S	Eq. (6), Transit 2 $\Delta v_D'$=2.205 km/s	23,042
m_T	A07	32,440
m_{TOT}	Eq. (1)	356,819

capability at this point is obtained by solving Eq. (7) for Δv.

$$m_{TOT} = (m_{TOT} - m_P)\exp(\Delta v / v_X) \tag{7}$$

Substituting m_{TOT}=198,468 kg, and m_P=11,757 kg from Table 7, together and v_X=8.826 km/s per A05, the desired Eq. (7) solution is Δv=0.539 km/s. Normalizing this surplus to the Δv actually expended during Transit 3 produces a margin of +0.539/4.437 = +12.1%, well in excess of the 5% per A22. Excess m_P margin in the Transit 3 worst case arises from conservative assumptions used to solve Eqs. 3 and 4. If assessment of Transit 3 did not

Table 5
Depletion of the Table 4 departure baseline is assessed for Transit 1. Values in the rightmost three columns are masses immediately after the corresponding events in the leftmost column. Radiation shielding in the Hab is at least RP5 when the rightmost column is positive.

Event	*T* (days)	Δv (km/s)	m_{LS} (kg)	m_P (kg)	m_{TOT} (kg)	$m_P + m_S - m_J$ (kg)
Perigee Lowering	0	0.242	24,953	136,692	347,168	+72,680
TMI	1	1.116	24,855	95,468	305,846	+31,456
MOI	204	1.586	4837	48,456	238,816	−15,555
Deimos Rendz.	204	0.751	4837	28,976	219,336	−35,036

Table 6
Depletion of the Table 4 departure baseline is assessed for Transit 2. Values in the rightmost three columns are masses immediately after the corresponding events in the leftmost column. Radiation shielding in the Hab is at least RP5 when the rightmost column is positive.

Event	T (days)	Δv (km/s)	m_{LS} (kg)	m_P (kg)	m_{TOT} (kg)	$m_P+m_S-m_J$ (kg)
Deimos Sep.	0	0.652	24,953	120,934	331,410	+56,922
TEI	0	1.553	24,953	67,462	277,938	+3450
TLI	237	0.935	1583	41,873	228,978	−22,138
LOI	240	0.378	1287	32,286	219,095	−31,726
SDRO Rendz.	240	0.309	1287	24,748	211,558	−39,264

Table 7
Depletion of the Table 4 departure baseline is assessed for Transit 3. Values in the rightmost three columns are masses immediately after the corresponding events in the leftmost column. Radiation shielding in the Hab is at least RP5 when the rightmost column is positive.

Event	T (days)	Δv (km/s)	m_{LS} (kg)	m_P (kg)	m_{TOT} (kg)	$m_P+m_S-m_J$ (kg)
TEIa	0	0.109	24,953	141,963	352,439	+77,952
TEIb	2	0.208	24,756	133,759	344,038	+69,748
TEIc	3	0.488	24,657	115,258	325,439	+51,247
TMI	6	0.891	24,362	84,037	293,922	+20,026
MOI	241	1.940	1188	30,612	217,323	−33,400
Deimos Rendz.	241	0.801	1188	11,757	198,468	−52,254

deplete m_{LS} in accord with (Eqs. (3) and 4) assumptions, Table 7's final m_P value would be reduced to 5358 kg, Eq. (7) would produce Δv=0.222 km/s, and the normalized m_P margin would be 5.0%.

As expected, Table 6 indicates Transit 2 has the slimmest margin with respect to RP5 radiation shielding for Transits 1–3 after Δv_D is expended. Post-TEI, the water mass shielding margin is but +3450 kg above m_J=87,053 kg. But the margin is +3450/87,053=+4.0% in this worst case. Shielding to better than RP5 is therefore provided until Transit 2 arrives at Earth per A03.

Care must be taken when applying (Eqs. (5) and 6) to assumptions differing significantly from those in Section 2. For example, imagine progressive decreases to I_{SP}=900 s adopted in A05. Below I_{SP}=658 s, Eq. (6) returns $m_S<0$. This result means decreased propulsion efficiency requires an m_P increase to the point *dedicated* shielding mass is not necessary. Under this condition, Eq. (3) can be solved for m_P while assuming m_S is zero. The resulting Eq. (8) then replaces Eq. (5), with m_S=0 replacing the otherwise negative value from Eq. (6).

$$m_P = \frac{m_Z(A-1)}{1 + (c_{RCS} + c_T)(1-A)} \tag{8}$$

As I_{SP} is further decreased to 309 s, Eq. (8)'s denominator approaches zero and nearly infinite m_P is computed. Below 309 s, $m_P<0$ is obtained from Eq. (8), indicating propulsive efficiency is incapable of achieving 1.05 $\Delta v'$ even with infinite m_P.

To illustrate the criticality of propulsive efficiency for *Aquarius*, consider the single change of I_{SP} from 900 s in A05 to 450 s while retaining all other Section 2 assumptions. This change increases m_P from 146,343 kg in Table 4 to 542,625 kg. Likewise, m_{TOT} increases from 356,819 kg in Table 4 to 832,176 kg. Per B04, the number of 130 t IMLEO launches required to assemble *Aquarius* jumps from 7.14 to 16.64.

5. *Aquarius* abort capability example

As an example of *Aquarius* contingency operations, suppose an abort targeting Earth return is necessary following Transit 3 TMI.

Table 8
When evolved to a precision Earth return trajectory, the patched conic abort solution corresponding to Fig. 14's Cell L33 is shown to be 2.7% pessimistic with respect to the $\Delta v_R+\Delta v_C \le 3.999$ km/s post-TMI viable abort capability criterion.

Trajectory	Δv_R (km/s)	Δv_C (km/s)	$\Delta v_R+\Delta v_C$ (km/s)
Patched Conic	3.842	0.153	3.995
Precision	3.721	0.169	3.890

Assuming full NTP functionality post-abort, Table 7 indicates m_P=84,037 kg of usable water propellant is available post-TMI in Transit 3. In a contingency, dedicated water shielding mass m_S=23,042 kg from Table 4 would presumably be added to produce an abort propellant mass budget $m_B=m_P+m_S$= 107,079 kg. Ignoring depletion of m_{LS} after TMI as a simplifying and conservative assumption, the rocket equation governing abort follows.

$$m_{TOT} = (m_{TOT} - m_B)\exp(\Delta v/v_X) \tag{9}$$

With m_{TOT}=293,922 kg from Table 7, and v_X=8.826 km/s per A05, Eq. (9) can be solved for Δv to produce a Transit 3 post-TMI *Aquarius* abort capability of 3.999 km/s.

The abort trajectory profile utilizes two NTP burns. The first burn has change-in-velocity magnitude Δv_R and reverses nominal motion away from Earth to initiate return. Per B03, Δv_R targets an Earth flyby with perigee height of +7700 km. When *Aquarius* reaches this perigee, a second purely retrograde burn with change-in-velocity magnitude Δv_C achieves Earth capture into an EEPO with apogee radius near 400,000 km. Assuming ECLSS systems and consumables have not been severely compromised, an orbit like this will permit the crew to remain aboard *Aquarius* while they await rescue. This or a similar orbit should also support whatever *Aquarius* repair or salvage operations are possible following abort.

Fig. 14 represents a matrix of Transit 3 patched conic abort trajectory solutions with the sum $\Delta v_R+\Delta v_C$ for a particular solution tabulated in each matrix cell. Thus, Cell L33 represents an abort initiated from the nominal Transit 3 trajectory with Δv_R performed on 20 November 2026 and Δv_C performed 14 April 2027. The sum $\Delta v_R+\Delta v_C$ for Cell L33 is a marginal 3.995 km/s. All Fig. 14 cells with $\Delta v_R+\Delta v_C \le 3.999$ km/s are colored **green**, indicating the corresponding abort trajectories are within *Aquarius* capability post-TMI. Those cells not satisfying this condition are colored **red**.

Viable abort cases in Fig. 14 typically expend less than 5% of the tabulated total Δv when achieving EEPO with Δv_C. The majority of abort Δv is required to reverse motion away from Earth with Δv_R in order to intercept Earth months later. This "slow return" attribute is compounded when the abort date is delayed. In Fig. 14, note the earliest viable Earth return date (corresponding to the uppermost green cell in a given column) is typically delayed 10 days for every day the abort date is delayed.

Fig. 14 indicates the Transit 3 point of no return is reached on 20 November 2026, about 13 days after TMI. Using Cell L33 as an

◇	A	B	C	D	E	F	G	H	I	J	K	L	M
1	**Earth Return**						**Aquarius Abort Date**						
2	**Date**	11/10/26	11/11/26	11/12/26	11/13/26	11/14/26	11/15/26	11/16/26	11/17/26	11/18/26	11/19/26	11/20/26	11/21/26
3	11/15/26	6.524	8.574	12.454	21.202	49.911							
4	11/20/26	5.072	5.681	6.506	7.649	9.294	11.783	15.809	22.992	38.141	85.157		
5	11/25/26	4.626	4.946	5.357	5.857	6.481	7.269	8.287	9.631	11.460	14.036	17.834	23.801
6	11/30/26	4.409	4.621	4.876	5.177	5.532	5.951	6.449	7.049	7.778	8.678	9.806	11.246
7	12/5/26	4.276	4.427	4.608	4.816	5.055	5.327	5.639	5.997	6.411	6.892	7.457	8.126
8	12/10/26	4.186	4.300	4.436	4.591	4.766	4.963	5.182	5.428	5.705	6.016	6.369	6.771
9	12/15/26	4.123	4.211	4.317	4.439	4.575	4.725	4.891	5.075	5.277	5.501	5.749	6.025
10	12/20/26	4.077	4.146	4.232	4.330	4.439	4.560	4.692	4.836	4.994	5.166	5.354	5.559
11	12/25/26	4.042	4.097	4.167	4.248	4.339	4.439	4.547	4.665	4.793	4.931	5.081	5.244
12	12/30/26	4.012	4.057	4.115	4.184	4.260	4.345	4.436	4.535	4.642	4.758	4.882	5.015
13	1/4/27	3.987	4.023	4.072	4.130	4.196	4.269	4.347	4.432	4.524	4.622	4.728	4.841
14	1/9/27	3.966	3.995	4.036	4.087	4.144	4.207	4.275	4.350	4.430	4.515	4.607	4.705
15	1/14/27	3.949	3.972	4.007	4.051	4.101	4.157	4.217	4.283	4.354	4.430	4.512	4.598
16	1/19/27	3.935	3.953	3.983	4.021	4.066	4.116	4.170	4.230	4.294	4.363	4.436	4.514
17	1/24/27	3.923	3.937	3.963	3.997	4.037	4.082	4.132	4.186	4.244	4.307	4.375	4.446
18	1/29/27	3.912	3.922	3.944	3.975	4.011	4.052	4.098	4.148	4.202	4.260	4.323	4.390
19	2/3/27	3.902	3.908	3.928	3.955	3.988	4.026	4.068	4.115	4.165	4.220	4.279	4.341
20	2/8/27	3.893	3.897	3.913	3.938	3.968	4.003	4.043	4.086	4.134	4.186	4.241	4.301
21	2/13/27	3.885	3.887	3.901	3.923	3.951	3.984	4.021	4.062	4.108	4.157	4.210	4.267
22	2/18/27	3.878	3.878	3.890	3.910	3.936	3.967	4.002	4.042	4.085	4.132	4.183	4.238
23	2/23/27	3.872	3.869	3.880	3.898	3.922	3.952	3.985	4.023	4.065	4.111	4.160	4.214
24	2/28/27	3.865	3.861	3.870	3.887	3.909	3.937	3.969	4.006	4.046	4.091	4.139	4.191
25	3/5/27	3.859	3.853	3.860	3.875	3.897	3.923	3.954	3.990	4.029	4.073	4.120	4.171
26	3/10/27	3.852	3.845	3.851	3.865	3.885	3.910	3.941	3.975	4.013	4.056	4.102	4.153
27	3/15/27	3.847	3.838	3.842	3.855	3.874	3.898	3.928	3.961	3.999	4.041	4.086	4.136
28	3/20/27	3.841	3.830	3.833	3.845	3.863	3.886	3.915	3.948	3.985	4.026	4.071	4.121
29	3/25/27	3.834	3.822	3.824	3.834	3.851	3.874	3.902	3.934	3.971	4.012	4.057	4.106
30	3/30/27	3.826	3.813	3.813	3.823	3.839	3.861	3.888	3.920	3.956	3.997	4.041	4.090
31	4/4/27	3.817	3.802	3.801	3.810	3.825	3.847	3.873	3.905	3.941	3.982	4.026	4.075
32	4/9/27	3.807	3.790	3.788	3.795	3.810	3.831	3.858	3.889	3.925	3.966	4.011	4.060
33	4/14/27	3.793	3.775	3.771	3.778	3.793	3.814	3.840	3.872	3.908	3.950	3.995	4.044
34	4/19/27	3.775	3.755	3.751	3.757	3.772	3.793	3.821	3.853	3.891	3.933	3.979	4.029
35	4/24/27	3.748	3.727	3.723	3.731	3.747	3.770	3.799	3.834	3.873	3.916	3.964	4.016
36	4/29/27	3.705	3.688	3.688	3.701	3.721	3.748	3.781	3.819	3.861	3.907	3.957	4.010
37	5/4/27	3.664	3.666	3.680	3.701	3.729	3.760	3.796	3.836	3.880	3.927	3.978	4.032
38	5/9/27	108.317	9.867	5.511	4.613	4.295	4.157	4.096	4.074	4.076	4.092	4.120	4.156
39	5/14/27	115.422	115.353	115.215	114.756	110.426	33.958	11.994	7.676	6.129	5.419	5.049	4.845

Fig. 14. Total abort Δv in km/s required to depart the nominal Transit 3 post-TMI trajectory and return to an EEPO is tabulated according to depart date (columns) and return date (rows). Row 2 and Column A provide these dates in mm/dd/yy format. Cells colored red require more total abort Δv than is available aboard *Aquarius* after Transit 3 TMI, while green-colored cells are viable abort opportunities. In Fig. 14 terminology, Transit 3 TMI occurs on 11/7/26. (For interpretation of the references to color in this figure legend, the reader is referred to the web version of this article.)

example abort on this date with the earliest viable Earth return, the patched conic solution is evolved to a precision trajectory with a pedigree matching those documented in Section 3. Results of this evolution are summarized in Table 8.

The precision trajectory's final approach to Earth and capture into an EEPO are plotted in Fig. 15. This EEPO is not at all conducive to *Aquarius* reuse because its ecliptic inclination is 85.6°, making access to SDRO-resident infrastructure difficult without major propulsive effort. Inclination with respect to Earth's true equator in the Fig. 15 EEPO is 64.6°, and near the minimum possible for this abort case in order to facilitate crew rescue. High inclinations challenging *Aquarius* reuse and her crew's rescue arise because geocentric v_∞ is only 0.6 km/s when *Aquarius* returns to Earth. Although this slow approach technique makes abort possible with available propellant as *Aquarius* nearly matches Earth's heliocentric orbit, it also tends to disproportionally magnify any deviations from this orbit during final Earth approach.

These potential difficulties must be considered before a specific abort case is addressed by returning *Aquarius* to the departure terminus of an interplanetary transit. It may be continuing onward to the destination terminus is a better course of action.

Using the water flow rate of 37.8 kg/s for NTP burns established at the end of Section 6, m_B=107,079 kg would require 47.2 min to burn in a Transit 3 maximum effort abort. Because the bulk of m_B is presumably consumed far from a transit terminus to achieve Δv_R, it could be split into multiple segments to remain within NTP duty cycle limits. But splitting the burn would not be an option during time-critical abort scenarios affecting NTP capability, such as a rapid water tank leak.

6. Additional work relating to the *Aquarius* proposal

Many of the assumptions cited in Section 2 are based on educated guesses, extrapolation, or pure speculation. Knowledge gaps relating to more critical functions in the *Aquarius* proposal are briefly discussed in the following paragraphs.

The RP5 specification in A03 reflects a point of diminishing returns documented in [16] (see Figs. 2–15 on p. 42), where proportionally greater ρ_A beyond 51.5 g/cm^2 is required to further shield a habitable volume. [16] data reflect a fixed 10 cm layer of water and a progressively thicker layer of aluminum. Diminishing ρ_A returns are largely due to incident radiation scattering (called spallation) by aluminum. How will spallation change if a 37 cm layer of water overlays Hab structure (presumably aluminum, per A12)? Will RP5 in the context of A01, A02, and B01 be an acceptable specification with respect to evolving interplanetary human spaceflight radiation dose standards?

Although NTP is the primary interplanetary human spaceflight propulsion system in NASA's [17] baseline, very little progress has been made since 1973 toward that end on technical, political, and diplomatic fronts ([13], Section 3.1). It should be noted the [17] NTP system uses liquid hydrogen as propellant to achieve I_{SP}=875–950 s ([17], p. 25). Is technical risk of nuclear reactor core temperatures well in excess of 3000 °C[14], necessary to "burn"

[14] Also noteworthy is that all existing experimental data on the disassociation of water into hydrogen and oxygen atoms has been obtained in furnaces, where the only energy governing this process is thermal. In a fission reactor core, gamma rays and neutrons supplement thermal energy. Determining the temperature at which water disassociates under exotic conditions in a fission reactor core requires

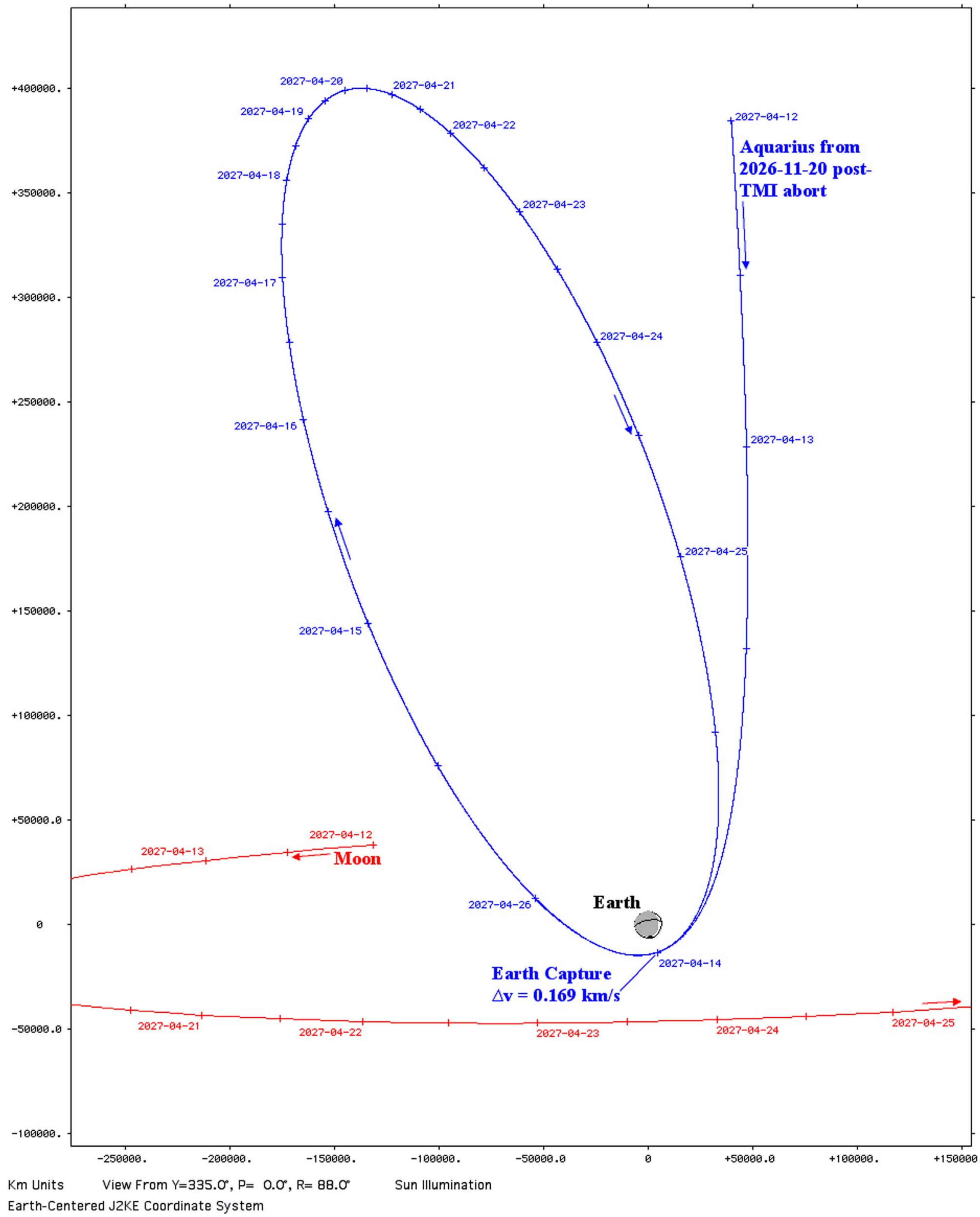

Fig. 15. Geocentric inertial motion of *Aquarius* (blue) and the Moon (red) are plotted as the spacecraft returns to Earth from a Transit 3 abort. The plot plane nearly coincides with the plane of *Aquarius* motion. Time tick labels are in yyyy-mm-dd format at 00:00 UT, and the shaded area is Earth's nightside. (For interpretation of the references to color in this figure legend,the reader is referred to the web version of this article.)

water propellant and achieve I_{SP}=900 s (per A05), a good trade against the potentially greater difficulties of refining, storing, and transporting liquid hydrogen, particularly in an ISRU context? How will spent fissile material aboard *Aquarius* be disposed of and replaced? If I_{SP}=900 s must be reduced, Fig. 16 shows the impact on

(*footnote continued*)
conducting new research. That temperature may be lower than we now suspect.

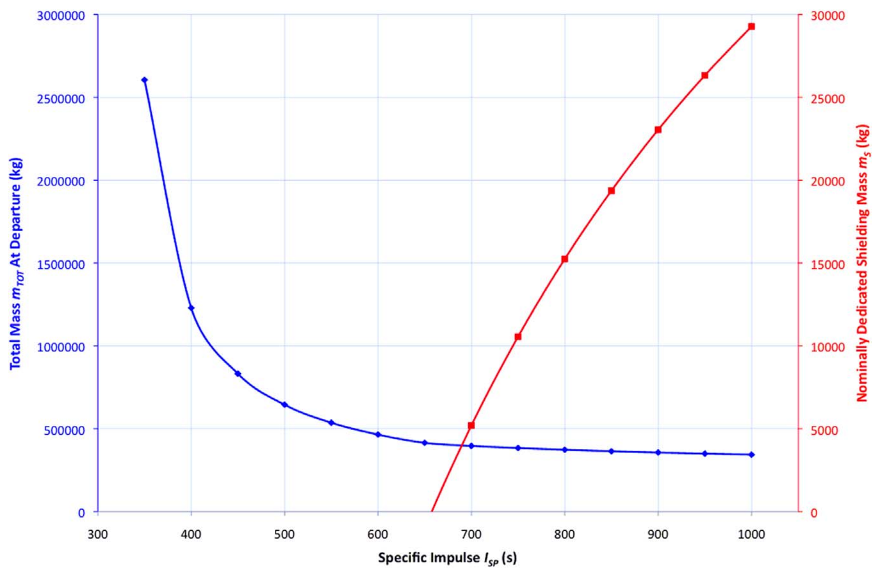

Fig. 16. The effects of NTP I_{SP} variations on m_S and m_{TOT} are plotted. At $I_{SP} < 658$ s, reduced NTP efficiency requires an increase in m_P to the degree that dedicating water mass as post-departure Hab radiation shielding (per A03) is not necessary, and $m_S = 0$.

m_S and m_{TOT} if all other Section 2 assumptions are preserved.

What "gravity prescription" will be used with the DAC's centrifuge per A16 ([13], Section 12.8)? Will crew time in the centrifuge required by that prescription in turn require radiation shielding from DAC structure be supplemented with a water jacket? Will DAC centrifuge crew conditioning during a return transit to SDRO infrastructure be sufficient to enable an Earth atmospheric entry at 11.0 km/s within 30 days (per B02), or will additional conditioning and loiter time in SDRO be necessary? A plan to develop the gravity prescription for crew readiness to withstand atmospheric entry from cislunar space after ~240 days in microgravity should be a major focus of centrifuge research with subjects confined to bed rest on Earth and aboard the International Space Station after it is equipped with a short-arm centrifuge.

Pre-positioned consumables and habitat in SDRO and at Deimos require masses in excess of 100 t be robotically transported over lunar and interplanetary distances (per B05 and B06). Robotic assembly in both locations and robotic excavation at Deimos will be necessary. Depending on whether or not ISRU is practical at or near these locations, mass transported from the Earth can be replaced by mass transported from the Moon or NEAs. Efforts to survey the Moon and a few NEAs for ISRU-pertinent materials are underway, but these need to be supplemented by surveys of Deimos and Phobos for ISRU material ([13], Table 13–6, p. 502 advocates such an ISRU survey of Phobos and Deimos as a high priority). Capability to robotically transport ~500 t of NEA material to SDRO is advocated in [15] via solar electric propulsion. This capability should also be applied to pre-positioning masses required to enable the *Aquarius* proposal.

7. Conclusions

From its inception in 1927, trans-Atlantic air transport has been a one-way proposition. Viable roundtrips are possible only because pre-emplaced return consumables are available for transport resupply at the destination. The *Aquarius* interplanetary transport proposed here has the same dependency.[15] Return consumables robotically pre-emplaced on Deimos, or cached on over a *thousand* occasionally more accessible NEAs, drastically reduce *Aquarius* total mass.

Because water is transported and stored over long time intervals in space with relative ease, its role as the primary *Aquarius* consumable poses no special obstacles to pre-emplacement logistics. The abundance of water on the Moon, Deimos, Phobos, and NEAs may virtually eliminate logistics from Earth through a combination of robotic ISRU and NEA material transport.

To serve as propellant at high efficiencies, water must be heated well above 3000 °C, where atomic disassociation begins to occur in thermal furnaces, and the system to accomplish this aboard *Aquarius* is assumed to be a nuclear reactor. This efficiency, together with return consumables pre-emplacement, reduces fully resupplied total *Aquarius* mass before an interplanetary departure to 357 t, about 90% of the assembled International Space Station's mass in March 2014.

Aquarius uses dedicated water mass and propellant residuals following interplanetary departure to shield much of her onboard habitable volume from radiation. Until interplanetary arrival propellant consumption begins, she provides her crew radiation shielding protection equivalent to at least 5% of that offered by Earth's atmosphere at sea level.

Because a large quantity of water mass must accompany *Aquarius* to shield her crew until an interplanetary arrival, burning that mass upon Earth return to permit her reuse is a logical consequence. Utilizing lunar orbit to garage and resupply *Aquarius* between roundtrips to Deimos has been demonstrated as a viable reuse strategy. Furthermore, flight profiles akin to those documented by this paper may be mandatory for crew survival if direct atmospheric entry poses unacceptable stress risks following an interplanetary roundtrip.

Aquarius is assembled in an elliptical Earth orbit with 2-day period and perigee above the inner Van Allen radiation belt. This orbit permits payload delivery about a day after launch and is thus able to capture the total energy deliverable by a cryogenic upper stage with great efficiency because long-term cryogenic storage is

[15] Both modes of transport have a performance dependency on pre-emplaced return consumables. It is arguable crew survival associated with interplanetary transport more critically depends on these consumables than does trans-Atlantic air transport. But such an argument must assume extended duration safe haven is not possible at Deimos in spite of B01 and B05.

avoided. Assuming 130 t IMLEO per launch, *Aquarius* can be assembled and readied for her maiden interplanetary transit with an estimated 7.14 launches. Thanks to her reusability, even complete resupply of propellant and crew consumables amounts to 185 t, 52% of *Aquarius* fully loaded total mass.

An abundance of water aboard *Aquarius* opens up potentially useful abort options. Even following an interplanetary departure with relatively large propellant consumption, a viable return to the departure planet is demonstrated for an abort initiated nearly two weeks after departure.

In 1954, the U.S.S. *Nautilus* was christened as the world's first nuclear-powered submarine. This paper's findings indicate a similar effort is necessary to achieve viable and sustainable interplanetary human transport. Admiral Hyman G. Rickover, who planned and personally supervised *Nautilus* construction, had appropriate advice for development of *Aquarius*. "The Devil is in the details, but so is salvation."

References

[1] E.N. Parker, Shielding space travelers, Sci. Am. (2006) 40–47.
[2] G.D. Badhwar, Shuttle radiation dose measurements in the international space station orbits, Radiat. Res. 157 (1) (2002) 69–75.
[3] F.A. Cucinotta, M.H. Kim, V. Willingham, K.A. George, Physical and biological organ dosimetry analysis for international space station astronauts, Radiat. Res. 170 (1) (2008) 127–138.
[4] G. Reitz, et al., Astronaut's organ doses inferred from measurements in a human phantom outside the international space station, Radiat. Res. 171 (2009) 225–235.
[5] J.E. Mazur, et al., New measurements of total ionizing dose in the lunar environment, Sp. Weather 9 (7) (2011).
[6] P.B. Saganti, et al., Model calculations of the particle spectrum of the galactic cosmic ray environment: assessment with ACE/CRIS and MARIE measurements, Radiat. Meas. 41 (2006) 1152–1157.
[7] C. Zeitlin, D.M. Hassler, F.A. Cucinotta, et al., Measurements of energetic particle radiation in transit to mars on the mars science laboratory, Science 340 (2013) 1080–1084.
[8] D. Hassler, et al., Mars' surface radiation environment measured with the mars science laboratory's curiosity rover, Science 343 (2014) 6169.
[9] J.L. Parsens, L.W. Townsend, Interplanetary crew dose rates for the August 1972 solar particle event, Radiat. Res. 153 (2000) 729–733.
[10] R.W. Orloff, D.M. Harland, Apollo: The Definitive Sourcebook, Springer-Praxis, Chichester, UK, 2006.
[11] J.B. Hopkins, Deimos and Phobos as destinations for human exploration, Lockheed-Martin Corporation 2013. (accessed 23.02.14) ⟨http://www.csc.caltech.edu/talks/hopkins.pdf⟩.
[12] D.R. Adamo, Trajectory challenges faced by reusable infrastructure in earth orbit supporting multiple departures for Mars, Space Show. Classr. (2013) ⟨http://spaceshowclassroom.files.wordpress.com/2013/11/multiplemarsdeparturesr1.pdf ⟩ (accessed 23.02.14).
[13] B.G. Drake, K.D. Watts, (ed.), Human Exploration of Mars Design Reference Architecture 5.0, NASA/SP-2009-566-ADD2, 2014. This document may be downloaded from ⟨http://www.nasa.gov/sites/default/files/files/NASA-SP-2009-566-ADD2.pdf⟩ (accessed 22.03.14).
[14] B.W. Barbee, Accessible Near-Earth Asteroids (NEAs), NASA, 2014, This document may be downloaded from ⟨http://www.lpi.usra.edu/sbag/science/NHATS_Accessible_NEAs_Summary.png ⟩ (accessed 23 February 2014).
[15] J. Brophy, F. Culick, L. Friedman, et al., Asteroid Retrieval Feasibility Study, Keck Institute for Space Studies, 2012, This document may be downloaded from ⟨ http://kiss.caltech.edu/study/asteroid/asteroid_final_report.pdf ⟩ (accessed 20.03.14).
[16] National Research Council Committee on the Evaluation of Radiation Shielding for Space Exploration, Managing Space Radiation Risk in the New Era of Space Exploration, The National Academies Press, 2008. This document may be downloaded from ⟨http://www.nap.edu/catalog.php?record_id=12045⟩ (accessed 24.02.14).
[17] B.G. Drake (ed.), Human Exploration of Mars Design Reference Architecture 5.0, NASA/SP-2009-566, 2009. This document may be downloaded from ⟨http://www.nasa.gov/exploration/library/esmd_documents.html⟩ (accessed 25.02.14).
[18] NASA/Boeing, U.S. Laboratory Module (Destiny), International Space Station (ISS) Interactive Reference Guide, Release 2.4, NASA, 2010. This document may be downloaded from ⟨http://www.nasa.gov/externalflash/ISSRG/pdfs/destiny.pdf⟩ (accessed 25.02.14).
[19] NASA, Volume I – Man-Systems Integration Standards, Revision B, NASA-STD-3000, NASA, 1995. This document may be downloaded from http://msis.jsc.nasa.gov/⟩ (accessed 26.02.14).
[20] D.L. Akin, Introduction to Space Life Support, University of Maryland, 2011, This document may be downloaded from ⟨http://spacecraft.ssl.umd.edu/academics/697S11/697S11L12.life_support.pdf ⟩.
[21] NASA/Boeing, U.S./Joint Airlock (Quest), International Space Station (ISS) Interactive Reference Guide, Release 2.4, NASA, 2010. This document may be downloaded from ⟨http://www.nasa.gov/externalflash/ISSRG/pdfs/quest.pdf⟩ (accessed 27.02.14).
[22] British Antarctic Survey, Mind the gap: space scientists uncover causes of gap in van allen belts, Science Daily, 2006. This document may be downloaded from ⟨http://www.sciencedaily.com/releases/2006/09/060926171157.htm⟩ (accessed 27.02.14).
[23] D.R. Adamo, A precision orbit predictor optimized for complex trajectory operations, AAS 03-665, Volume 116 of the Advances in the Astronautical Sciences, Univelt, San Diego, 2003, pp. 2567–2586.
[24] J. Meeus, Astronomical Algorithms, Willman-Bell, Inc., Richmond, VA, USA, 1991.
[25] J.D. Giorgini, D.K. Yeomans, A.B. Chamberlin, P.W. Chodas, R.A. Jacobson, M. S. Keesey, J.H. Lieske, S.J. Ostro, E.M. Standish, R.N. Wimberly, JPL's on-line solar system data service, Bull. Am. Astron. Soc. 28 (3) (1996) 1158 ⟨http://ssd.jpl.nasa.gov/?horizons⟩ (accessed 10.03.14).